

Biostratigraphy and facies around the D/C boundary interval of the Tuye-Darvar section, Eastern Alborz Range, NE Iran

Bioestratigrafía y facies en torno del intervalo del límite D/C de la sección Tuye-Darvar, Este de Montañas Alborz, NE de Irán

Elaheh Sattari¹, Ali Bahrami^{1,*}, Peter Königshof², Hossein Vaziri-Moghaddam¹, Azizollah Taheri⁴

¹ Department of Geology, Faculty of Sciences, University of Isfahan, Isfahan, Iran.

² Senckenberg, Research Institute and Natural History Museum, Senckenberganlage 25, 60325 Frankfurt am Main, Germany.

³ Faculty of Earth Sciences, Shahrood University of Technology, Shahrud, Iran.

* Corresponding author: (A. Bahrami) a.bahrami@sci.ui.ac.ir

How to cite this article:

Sattari, E., Bahrami A., Königshof, P., Vaziri-Moghaddam, H., Taheri A., 2024, Biostratigraphy and facies around the D/C boundary interval of the Tuye-Darvar section, Eastern Alborz Range, NE Iran: Boletín de la Sociedad Geológica Mexicana, 76 (1), A280224. <http://dx.doi.org/10.18268/BSGM2024v76n1a280224>

Manuscript received: January 1, 2024.
Corrected manuscript received: February 20, 2024.
Manuscript accepted: February 29, 2024.

Peer Reviewing under the responsibility of Universidad Nacional Autónoma de México.

This is an open access article under the CC BY-NC-SA license (<https://creativecommons.org/licenses/by-nc-sa/4.0/>)

ABSTRACT

The 1st order mass extinction at the Devonian/Carboniferous transition, known as the Hangenberg Crisis, is characterized by major transgressive/regressive cycles which led to widespread ocean anoxia during the Hangenberg Black Shale Event, as well as to a global major sea-level fall and the worldwide deposition of regressive Hangenberg Sandstone equivalents. The Devonian/Carboniferous transition at the Tuye-Darvar section in the eastern Alborz Range is studied in terms of conodont biostratigraphy, litho-, microfacies and sequence stratigraphy. In order to examine the biostratigraphical framework, forty conodont samples were systematically taken from the studied interval. Thirty-two conodont species belonging to ten genera led to the discrimination of twelve conodont zones, ranging from the *Pseudopolygnathus granulatus* Zone to the *Scaliognathus anchoralis-Doliognathus latus* Zone. Due to facies, the conodont record also exhibits some hiatuses. Field observations and sedimentological and microfacies studies led to the identification of thirteen facies types from sub-tidal environments to the fully marine environments, including seven microfacies types. The sediments deposited in a mixed carbonate-siliciclastic platform, revealed four third-order sequences. The Hangenberg Black Shale is not recorded in the Tuye-Darvar section as a result of depositional facies. In comparison with other studied Devonian/Carboniferous Boundary (DCB) sections of the central and northern Iran, the Tuye-Darvar section suggests a tectonic position, which is most likely placed on a separate tectonic block.

Keywords: Mixed carbonate-siliciclastic platform, sequence stratigraphy, D/C boundary, conodont biostratigraphy.

RESUMEN

La extinción de 1er orden en la transición Devónico/Carbonífero, conocida como la Crisis Hangenberg, se caracteriza por ciclos mayores transgresivos/regresivos, los cuales llevaron a una extensa anoxia oceánica durante el Evento Hangenberg de Lutita Negra, así como a un descenso global del nivel del mar y el depósito regresivo equivalente de la Arenisca Hangenberg. La transición Devónico/Carbonífero en la sección Tuye-Darvar ubicada en la región Este de las Montañas Alborz es estudiada en términos de bioestratigrafía de conodontos, lito-, microfacies is studied in terms of conodont biostratigraphy, litho-, microfacies y estratigrafía de secuencias. Con el propósito de examinar el marco bioestratigráfico, cuarenta muestras de conodontos fueron tomadas sistemáticamente del intervalo estudiado. Treinta y dos especies de conodontos, pertenecientes a diez géneros condujeron a la discriminación de doce zonas de conodontos, cubriendo de la Zona de *Pseudopolygnathus granulatus* a la Zona de *Scaliognathus anchoralis-Doliognathus latus*. Debido al tipo de facies, el registro de conodontos presenta algunos hiatus. Observaciones de campo y estudios sedimentológicos y de microfacies, permitieron la identificación de trece tipos de facies, de ambientes subtidales a ambientes completamente marinos, incluyendo siete tipos de microfacies. The sediments deposited in a mixed carbonate-siliciclastic platform, revealed four third-order sequences. The Hangenberg Black Shale is not recorded in the Tuye-Darvar section as a result of depositional facies. En comparación a otros Límites Devónico/Carbonífero (LDC) estudiados en el Norte y Centro de Irán, la sección Tuye-Darvar sugiere una posición tectónica, muy probablemente ubicada en un bloque tectónico separado.

Palabras clave: Plataforma carbonato-siliciclástica mixta, estratigrafía de secuencias, límite D/C, estratigrafía de conodontos.

1. Introduction

The Devonian/Carboniferous (D/C) transition is characterized by several transgressive/regressive (T/R) cycles and widespread ocean anoxia have been recognized along continental margins or epicontinental basins known as the Hangenberg Black Shale Event (HBS) (Bahrami *et al.*, 2011b, 2022; Sattari *et al.*, 2023). Close to the Devonian Carboniferous boundary (DCB) a major sea-level fall (Hangenberg Sandstone Event, HSS) of assumed more than 100 m (Kaiser and Corradini, 2011; Myrow *et al.*, 2014 see summary in Kaiser *et al.*, 2016; Salehi *et al.*, 2020), which is most likely associated with the glaciation on Gondwana (*e.g.* Isaacson *et al.*, 1999, 2008; Streef *et al.*, 2000a, 2000b; Caputo *et al.*, 2008; Brezinski *et al.*, 2010; Lakin *et al.*, 2016) can be recognized in many sections around the world. The deposition of these black shales and sandstones is known as the early and middle phase of the Hangenberg Crisis as defined by Kaiser *et al.* (2016) and Becker *et al.* (2016). Stratigraphical gaps and non-deposition related to this major regression are also known from eastern Iran as it was shown by Bahrami *et al.* (2011b). Most of the DCB sections from the central and eastern Alborz Range have been deposited in a shallow-water, carbonate ramp setting (Bahrami *et al.*, 2019, 2022; Königshof *et al.*, 2021; Parvizi *et al.*, 2021).

The Alborz Range and the adjacent central Iran microplate represent remnants of the Early Palaeozoic passive margin of Gondwana, which underwent an important rifting phase during the Ordovician to Silurian time span (Stöcklin, 1968; Stöcklin, 1974; Berberian and King, 1981; Şengör *et al.*, 1988). The Ordovician-Silurian rifting phase followed by renewed continental shelf deposition from the Middle Devonian to the Middle Triassic. During this time-span, Iran was located in the northern margin of Gondwana, along the southern border of the Palaeo-Tethys Ocean (Golonka, 2007; Bagheri and Stampfli, 2008; Bahrami *et al.*, 2015). The Alborz Range was an extensive continental shelf during the

Middle Devonian to the Middle Triassic, when the Alborz-Central Iran zones collided with Eurasia, generating siliciclastic sediments from continental to marine facies, including different carbonates ranging from shallow-marine to deeper marine settings (Stöcklin, 1974; Clark *et al.*, 1975; Berberian and King, 1981; Alavi, 1996; Stampfli *et al.*, 2001; Wendt *et al.*, 2005) (Figure 1).

In other zones of Iran, specially the Central Iran Zone, studies have also been conducted in the Middle/Late Devonian and early Carboniferous deposits based on conodont fauna (Boncheva *et al.*, 2007; Bahrami *et al.*, 2011a, 2013, 2014a, 2014b, 2017, 2020, Königshof *et al.*, 2017; Zamani *et al.*, 2021). In addition to conodonts, other fossil groups, for example bryozoans, have also been studied in the Late Devonian in Iran (Ernest *et al.*, 2016, 2020).

The D/C transition in the Eastern Alborz Range of the Tuye-Darvar section, is composed of the Jeirud Formation (Upper Devonian) and Mobarak Formation (Lower Carboniferous). Previous studies from this section have focused on sedimentology, and trace fossil analysis (Sharafi *et al.*, 2014, 2016). However, few biostratigraphic studies have been conducted on conodonts (Najjarzadeh, 1998; Najjarzadeh *et al.*, 2020), but combined biostratigraphic and sedimentologic/facies analysis is still lacking.

This study presents new biostratigraphic data, an improved sedimentological/facies description of the Tuye-Darvar section, and thus it is an important contribution to ongoing discussions on the D/C boundary (see Aretz and Corradini, 2021).

2. Geological Setting

The Alborz Mountains are over 2000 km long and are strongly affected by the subduction of Palaeo-Tethyan and collision between the Iranian block of Gondwana and the Turan plate in the southern margin of Laurasia (Alavi, 1991; Muttoni *et al.*, 2009). It is bounded by the Palaeo-Tethys

collisional suture zone in the north and northeast, by the Caspian depression in the northwest, and by the Kopet-Dagh Zone in the east (Alavi, 1996; Nogol-e-sadat and Almasian, 1993). According to tectono-stratigraphic studies (Stöcklin, 1974; Alavi, 1991, 1996), the Alborz Range is subdivided into south central, north central, and the Anti-Alborz.

The Tuye-Darvar section is located 35 km southwest of Damghan city, adjacent to Darvar village (base of the section: 36° 01' 27.31" N, 53° 53' 17.33" E; top of the section: 36° 01' 19.32" N, 53° 53' 33.03" E (Figure 2). The studied section has a thickness of 248 meters and contains the Jeirud- and Mobarak formations. For the first time, the Jeirud and Mobark formations were described by Assereto (1963) as a shallow-marine succession in the Alborz Range. In the studied area, the Jeirud Formation is mostly composed of siliciclastic sediments, which overlies the? Late Cambrian-Early Ordovician Mila Formation. The Devonian/Carboniferous boundary corresponds

to the base of last sandstone horizon at the base of the first limestone unit of the Mobarak Formation. The limestones of the Mobarak Formation covered by the Triassic Elika Formation.

3. Methods and material

In order to improve and update the biostratigraphic framework of the Tuye-Darvar section forty conodont samples of approximately 5 to 8 kg each were taken from carbonate rock and processed by standard methods (see Jeppsson and Anehus, 1995). The process was repeated until samples were dissolved. The washed residues were dried in an oven (~ 40 °C) and later sieved and separated into different fractions. The nominated conodonts and related biozones were distinguished, using revised conodont zones (e.g Spalletta *et al.*, 2017 and Becker *et al.*, 2021). Also 210 thin sections and polished slabs were used for sedimentologic and microfacies

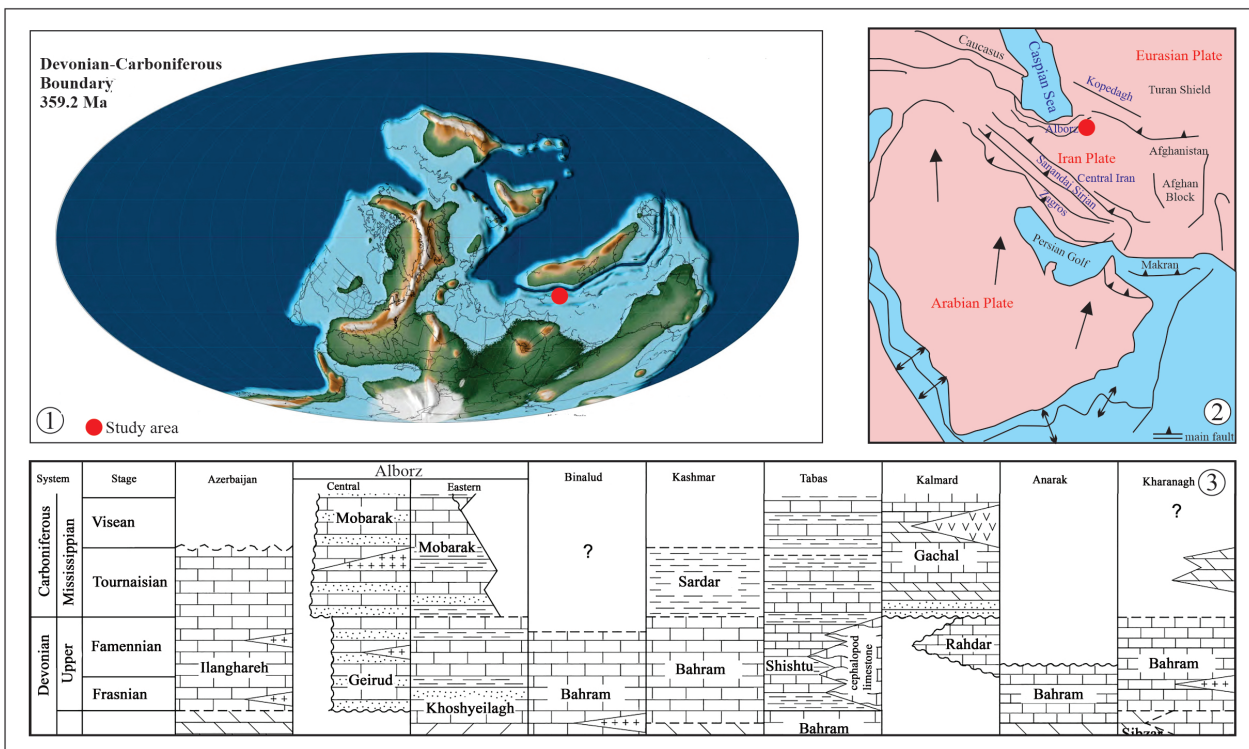


Figure 1 (a) Paleogeographic reconstruction map (modified after Scotese, 2001) showing the location of the investigated area and (b) Tectonic map of the Iran region, after Sorkhabi and Macfarlane (1999), (c) Synoptic view of Upper Devonian to Carboniferous formations in Iran (modified from Wendt *et al.*, 2005).

analysis. For sedimentological description, we follow the Dunham (1962) and Embry and Klovan (1971) classifications for carbonate rocks and were compared with other facies models, such as Flügel (2010). The petrographic description of the sandstones follows Pettijohn *et al.* (1987). The mud rocks classification follows the scheme of Dorrik (2010). For sequence stratigraphic interpretation, we follow the concepts by Emery and Myers (1996), and Catuneanu *et al.* (2005, 2009).

4. Lithostratigraphy

4.1. JEIRUD FORMATION

The Jeirud Formation is 166 m thick, and is composed of six lithostratigraphic units described from base to top as follows:

The Jeirud Formation disconformably overlies the green shales of the? Late Cambrian-Early Ordovician (Mila Formation) (Figure 3a):

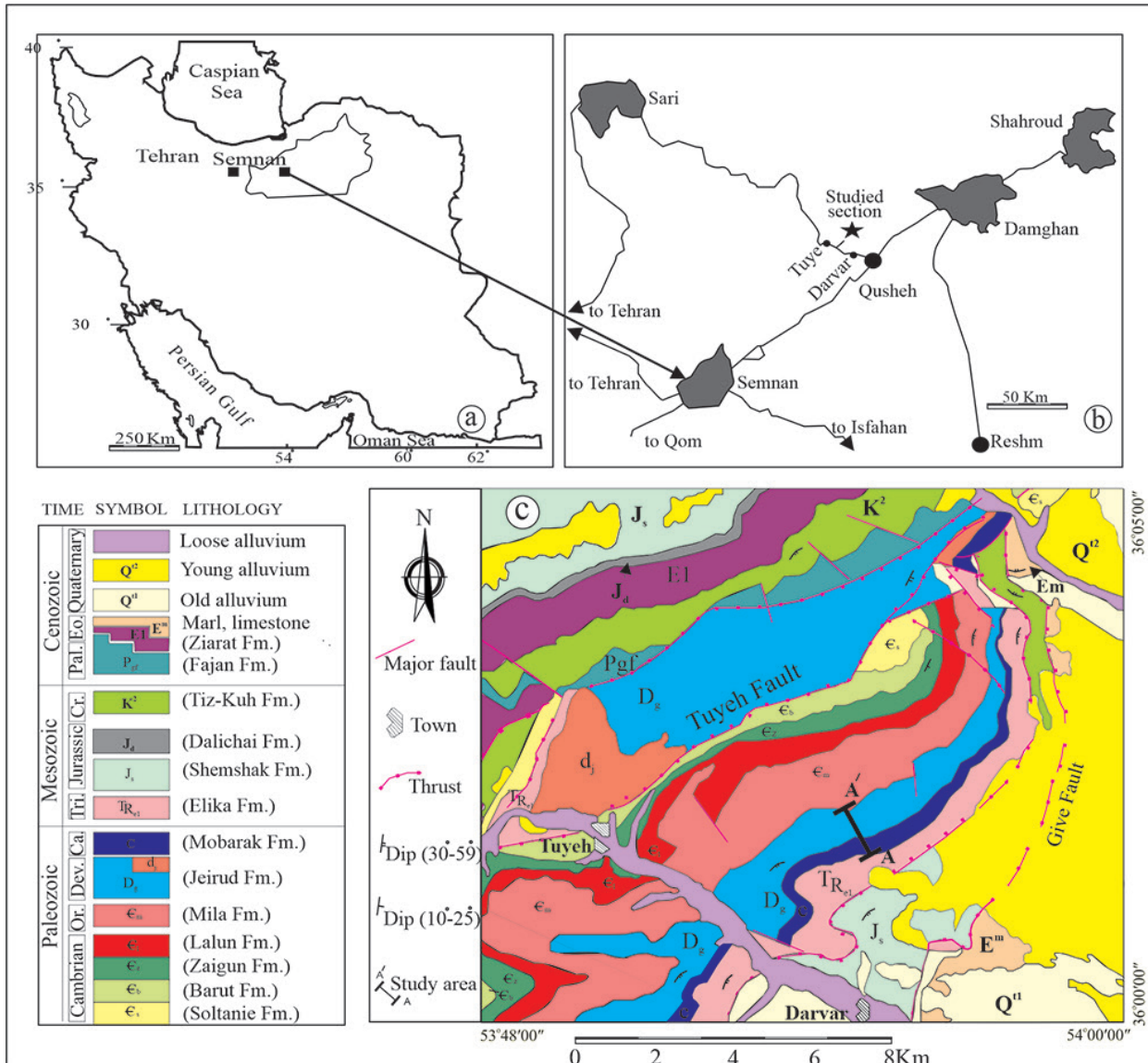


Figure 2 (a) and (b) Geographical location and access routes to the studied section (Bakhtiari, 2005), (c) Geological map of the study area, taken from the Kiasar Map of 1/100,000 (modified after Saidi and Akbarpour, 1992).

- Unit 1 (27.5 m) consists of thin to thick-bedded light grey sandstone with green shale interlayers and to a lesser extent red sandstone and shale. The sedimentary structures are chevron cross-bedding and parallel lamination. At least two upward shallowing cycles are obvious in this unit (Figure 3b).
- Unit 2 (10.3 m) includes red conglomerate, an alternation of massive red sandstone (showing chevron cross-bedding and herringbone cross-bedding), and a red shale (Figure 3c).
- Unit 3 (46.2 m) consists of white sandstone and green shale interlayers. Sedimentary structures show chevron cross-bedding, flaser bedding, hummocky cross-stratification, and parallel lamination. Bivalve and echinoderm remains are the identified macrofossils in this interval (Figure 3d).
- Unit 4 (26.2 m) is composed of thick-bedded brown dolostone, an alternation of black shale and massive sandstone, showing trough cross-bedding, planar cross-bedding, and ripple marks (Figure 3e).
- Unit 5 (24.8 m) consists of an alternation of gray-black sandstones, black shale layers, and thin-bedded limestone, showing herringbone cross-bedding, chevron cross-bedding, and parallel lamination. Some fossil groups such as crinoids and brachiopods exhibit growth differences and were found in this succession (Figure 3f).
- Unit 6 (31 m) commences with a massive and very poorly sorted clast-supported microconglomerate, which is overlain by thin-bedded dark limestone. Intercalated are thin-bedded black shales and sandstone horizons showing hummocky cross-stratification (HCS). This unit is very fossiliferous and contains bryozoans, gastropods, ostracods, bivalves, corals, brachiopods, and crinoids, which occur preferably in the interbedded limestones.

4.2. MOBARAK FORMATION

The boundary between the Jeirud Formation and the Mobarak Formation is placed at the top of last sandstone horizon at the base of the first limestone unit of the Mobarak Formation. The

Mobarak Formation is unconformably overlain (fault) by the vermiculite limestones of the Elika Formation (Lower-Middle Triassic). Based on the field observation three lithostratigraphic units were identified:

Unit 1 (26 m) an alternation of thin-bedded, gray fossiliferous limestone and grey to dark shales.

Unit 2 (20 m) comprises shaly beds with interlayers of medium-bedded fossiliferous limestone.

Unit 3 (35.5 m) includes thick-bedded fossiliferous limestone with minor shale layers. This interval is fossiliferous and exhibits preferably crinoids, solitary corals, and brachiopods.

5. Biostratigraphy

Despite numerous conodont samples were taken, the total number of obtained conodont elements is rare, although most of the samples yielded conodonts and almost contained adequate material for biostratigraphic analysis.

All in all 158 revealed conodont elements led to the discrimination of twelve biostratigraphic intervals (Figures 4; 5 and 6, Table 1) and to the identification of thirty-two species and subspecies within ten genera. Overall, the preservation of the conodont elements is very good, the color alteration of conodonts (Epstein *et al.*, 1977) is CAI 4 - 4.5.

As the lower part of the section is primarily composed of sandstone and dolomite, the first conodont-bearing sample is S2 from the base of unit 5.

Although the pelagic conodont zonation cannot fully applied to the shallow-water settings which are, unfortunately, poor in conodonts and often lack index species, we have found enough diagnostic species to apply the conodont zonation proposed by Spalletta *et al.* (2017) and Becker *et al.* (2021). The stratigraphy ranges from the late Famennian and Early Mississippian.

Early Mississippian conodont stratigraphy also is based on publications by Sandberg *et al.* (1978), Lane *et al.* (1980), and Kaiser *et al.* (2017).

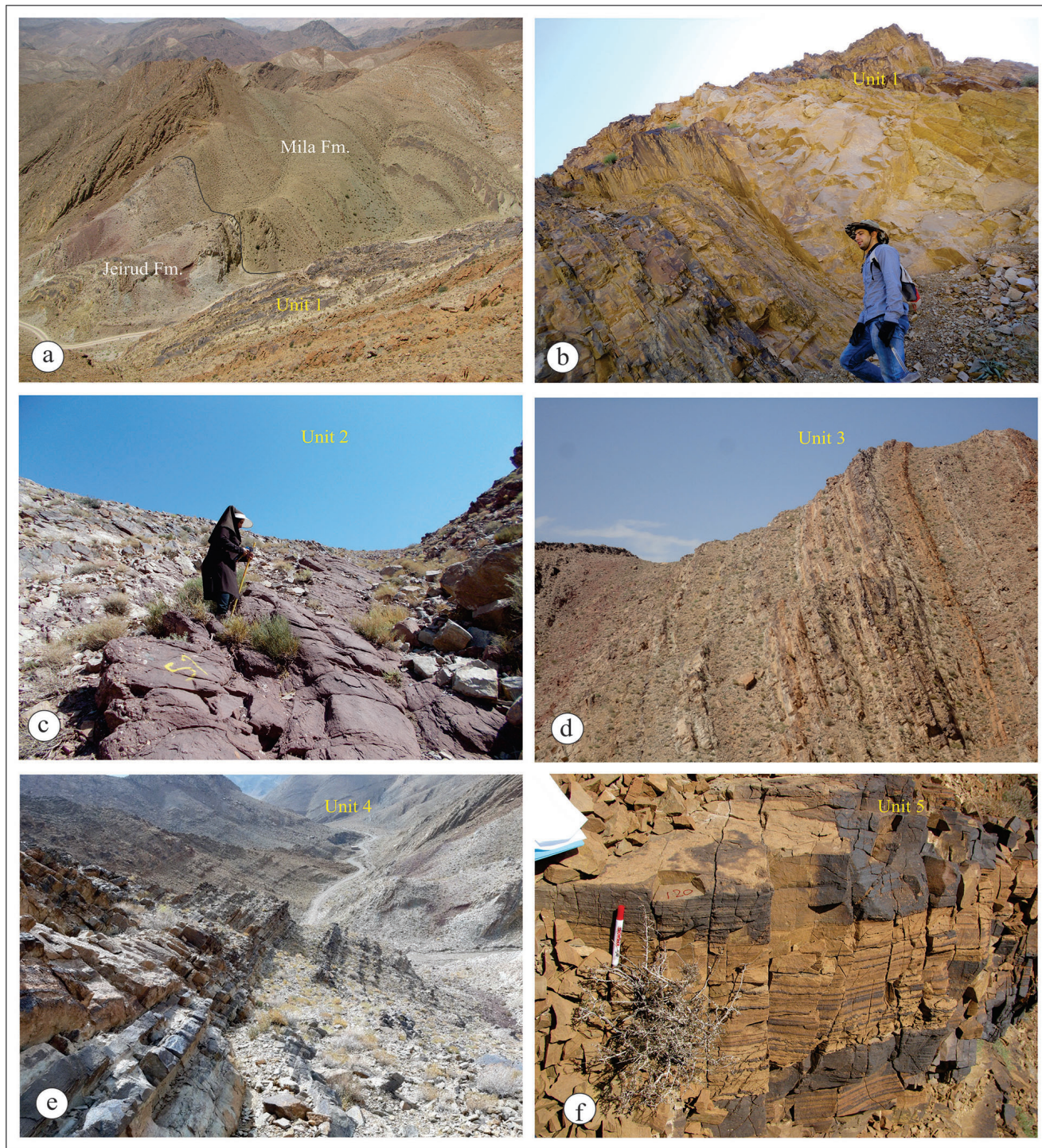


Figure 3 Lithostratigraphic units of the Tuye-Darvar Section: (a) The erosional contact of the Jeirud Formation with green shales of the Mila Formation, (b) Unit 1 of the Jeirud Formation (the dominant lithology of this unit is massive white quartz arenite sandstones), (c) The beginning of Unit 2 with red clast-supported and polygenetic conglomerate, (d) Unit 3 of the Jeirud Formation with the predominance of quartz arenite sandstones and non-laminated shaly interlayers, (e) Unit 4 alternation of sandstone, shale and dolomite, (f) Parallel laminations in the sandstones of the Unit 5.

Conodont zones/subzones were defined by the First Appearance Datum (FAD) of index species as well other marker species or assemblages occurring within given conodont zones.

5.1. PSEUDOPOLYGNATHUS GRANULOSUS ZONE (SAMPLE S2)

This conodont Zone (Spalletta *et al.*, 2017) was recognized at the lowermost part of unit 5 where the carbonate portion of the Jeirud Formation starts. It corresponds to the Upper *velifer* Zone of Ziegler (1962, 1969) and Late *trachytera* Zone of Ziegler and Sandberg (1990). The lower boundary of this narrow biozone is not defined in the section due to the lack of any index conodont species. The upper boundary is well defined due to the marker species *Polygnathus padovani*, *Palmatolepis minuta minuta* and *Scaphignathus velifer velifer*. All mentioned species become extinct at the end of *Ps. granulosis* Zone (Spalletta *et al.*, 2017). *Bispathodus stabilis stabilis* is another zonal indicator, which appears at the end of *Ps. granulosis* Zone is found in the sample.

5.2. POLYGNATHUS STYRIACUS ZONE (SAMPLE S3)

Polygnathus styriacus Zone (Spalletta *et al.*, 2017) is located within the lower part of unit 5, complies with the Lower *styriacus* Zone of Ziegler (1962, 1969) and Early *postera* Zone of Ziegler and Sandberg (1990). Although there is no index conodont species for defining the lower and upper boundary, this biozone is indicated based on associated conodont fauna such as *Bispathodus stabilis*, *Bispathodus stabilis bituberculatus* and *Polygnathus semicostatus*. This assemblage points to this biozone.

5.3. PALMATOLEPIS GRACILIS MANCA ZONE (SAMPLE S4)

Palmatolepis gracilis manca Zone (Spalletta *et al.*, 2017) matches with the Middle *styriacus* Zone of Ziegler (1962, 1969), and the Late *postera* Zone of Ziegler and Sandberg (1990) and falls within the

unit 5. The lower boundary is defined by the first appearance of *Bispathodus bispathodus* Ziegler *et al.* 1974. The upper boundary corresponds to the base of the next zone.

5.4. PALMATOLEPIS GRACILIS EXPANSA ZONE (SAMPLE S5)

This biozone (Spalletta *et al.*, 2017) is compatible with the Upper *styriacus* Zone of Ziegler (1962, 1969) and Early *expansa* Zone of Ziegler and Sandberg (1990) and corresponds to a grey, thin bedded limestone of unit 5. The lower boundary is defined by the first occurrence of *Bispathodus jugosus* Branson and Mehl, 1934a and *Pseudopolygnathus primus* Branson and Mehl, 1934b. The upper boundary corresponds to the next Zone. *Bispathodus stabilis vulgaris*, *Branmehla inornata*, *Polygnathus communis communis*, *Bispathodus bispathodus*, *Polygnathus semicostatus*, *Bispathodus stabilis stabilis* were also found in this sample.

5.5. BISPATHODUS ACULEATUS ACULEATUS ZONE (SAMPLE S6)

Bispathodus aculeatus aculeatus Zone (Spalletta *et al.*, 2017) corresponds to the Upper *styriacus* Zone of Ziegler (1962, 1969) and the Middle *expansa* Zone of Ziegler and Sandberg (1990). The lower boundary is defined by the first occurrence of species *Bispathodus aculeatus aculeatus* Branson and Mehl, 1934a, *Bispathodus spinulicostatus* Branson and Mehl, 1934a and *Clydagnathus plumulus* (Rhodes *et al.*, 1969). *Bispathodus stabilis bituberculatus* (Dzik, 2006) [M3] become extinct in this biozone. *Bispathodus stabilis stabilis*, and *Polygnathus delicatulus* are also present.

5.6. BISPATHODUS COSTATUS ZONE (SAMPLE S7)

This biozone (Spalletta *et al.*, 2017) matches with Lower *costatus* Zone of Ziegler (1962, 1969) and upper part of Middle *expansa* Zone of Ziegler and Sandberg (1990). The lower boundary is defined by the first occurrence of the zonal index species *Bispathodus costatus* [M2] Branson and Mehl,

1934a and the upper limit correspond to the next zone. *Clydagnathus plumulus*, *Bispathodus aculeatus aculeatus*, *Bispathodus stabilis vulgaris*, *Branmehla inornata*, *Bispathodus jugosus*, *Polygnathus communis communis*, *Bispathodus bispathodus*, *Pseudopolygnathus primus* M2, *Bispathodus stabilis stabilis* are the other accompanying species.

5.7. BISPATHODUS ULTIMUS ULTIMUS ZONE (SAMPLE S8- SAMPLE S9)

Bispathodus ultimus Zone (Kaiser *et al.*, 2009) occurs within the latest portion of unit 5 and the base of unit 6. This zone complies to the Middle *costatus* Zone of Ziegler (1962, 1969), and the upper part of Late *expansa* Zone of Ziegler and Sandberg (1990) and corresponds to the lower part of new erected *Bi. ultimus* Zone of Spalletta *et al.* (2017). The lower boundary is defined by the first occurrence of zonal index species *Bispathodus ultimus* [M1] and the upper limit is defined by the last occurrence of *Bispathodus costatus* [M2]. The following conodont taxa *Clydagnathus plumulus*, *Bispathodus spinulicostatus*, *Bispathodus aculeatus aculeatus*, *Bispathodus stabilis vulgaris*, *Branmehla inornata*, *Bispathodus jugosus*, *Polygnathus communis communis*, *Bispathodus bispathodus*, *Polygnathus semicostatus* are the accompanying species in this sample.

5.8. SIPHONODELLA (EOSIPHONODELLA) PRAESULCATA ZONE TO COSTATUS-KOCKELI INTERREGNUM ZONE (CKI) (SAMPLE S10-S13)

This biozone (Kaiser *et al.*, 2009) matches with the Upper *costatus* Zone of Ziegler (1962, 1969), the Early *praesulcata* Zone and partly the Middle *praesulcata* Zone of Ziegler and Sandberg (1990) and corresponds to the middle and upper part of new erected *Bi. ultimus* Zone of Spalletta *et al.* (2017). The lower boundary is defined by the first occurrence of *Siphonodella praesulcata* Sandberg (in Sandberg *et al.*, 1972), *Protognathodus meischneri* and *Protognathodus collinsoni* which have been found in this sample. The upper limit corresponds to the next Zone. *Pseudopolygnathus primus* M2, *Polygnathus communis dentatus* are the accompanying species.

5.9. PROTOGNATHODUS KOCKELI ZONE (SAMPLE S14-SAMPLE S15)

Protognathodus kockeli Zone (Kaiser *et al.*, 2009) corresponds to the Lower *Protognathodus* fauna of Ziegler (1962, 1969) and Late *praesulcata* Zone of Ziegler and Sandberg (1990). The lower boundary is defined by the first occurrence of *Protognathodus kockeli* and the upper limit by the first occurrence of *Siphonodella sulcata* at the base on the next biozone. *Protognathodus meischneri* and *Protognathodus collinsoni* occur in this sample, whereas *Protognathodus kockeli* was not found.

5.10. SIPHONODELLA (EOSIPHONODELLA) SULCATA S.L./PROTOGNATHODUS KUEHNI ZONE TO SIPHONODELLA (EOSIPHONODELLA) CRENULATA ZONE (SAMPLE S16-S25)

This conodont interval falls within the grey limestones of unit 1 and unit 2 at the base of Mobarak Formation (Early Mississippian). Unit 1 rests disconformably on unit 6, the topmost portion of the Jeirud Formation which is characterized by a thin layer of micro conglomerate. The lower boundary of this interval corresponds to the first occurrence of *Siphonodella sulcata* in sample S16 just above the DCB boundary. *Protognathodus meischneri*, *Protognathodus collinsoni*, *Protognathodus kockeli*, *Siphonodella praesulcata* Sandberg (in Sandberg *et al.*, 1972) are the other important indicator species at this interval. *Polygnathus longiposticus*, *Polygnathus inornatus inornatus*, *Polygnathus communis dentatus*, *Polygnathus communis communis*, *Bispathodus stabilis stabilis* are accompanying species in the sample.

5.11. SIPHONODELLA (S.) ISOSTICHA - U. SIPHONODELLA (S.) CRENULATA-GNATHODUS TYPICUS ZONES (SAMPLE 26-SAMPLE 35)

This bio-interval matches with the topmost part of unit 2 into near the top of unit 3, the lower boundary is defined by the first occurrence of *Gnathodus cueniformis*, *Gnathodus semiglaber*, *Gnathodus typicus*, and *Pseudopolygnathus multistriatus* at sample S26. The upper limit coincides to the beginning of the next Zone.

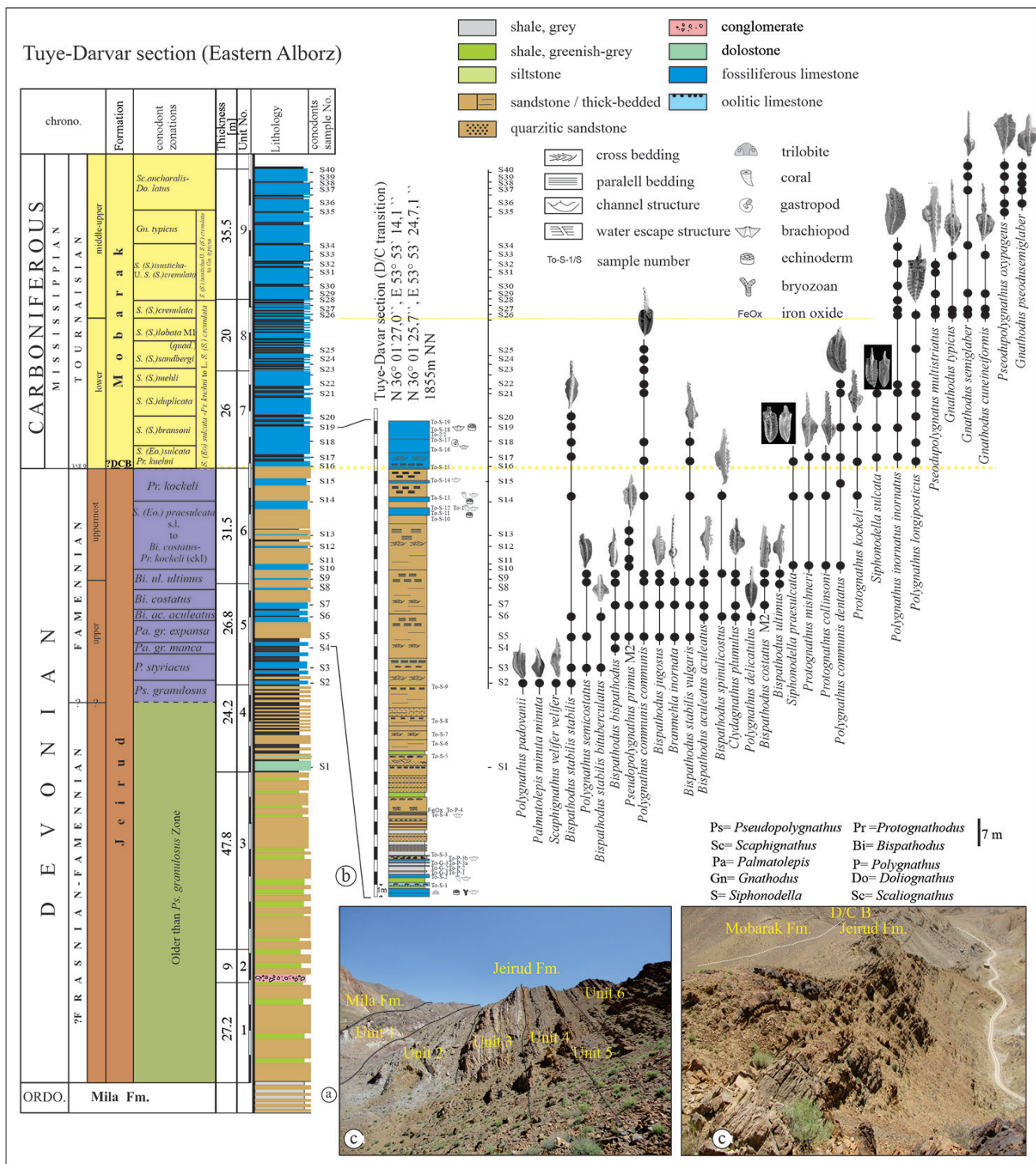


Figure 4 Lithological units and biozones of the studied section.

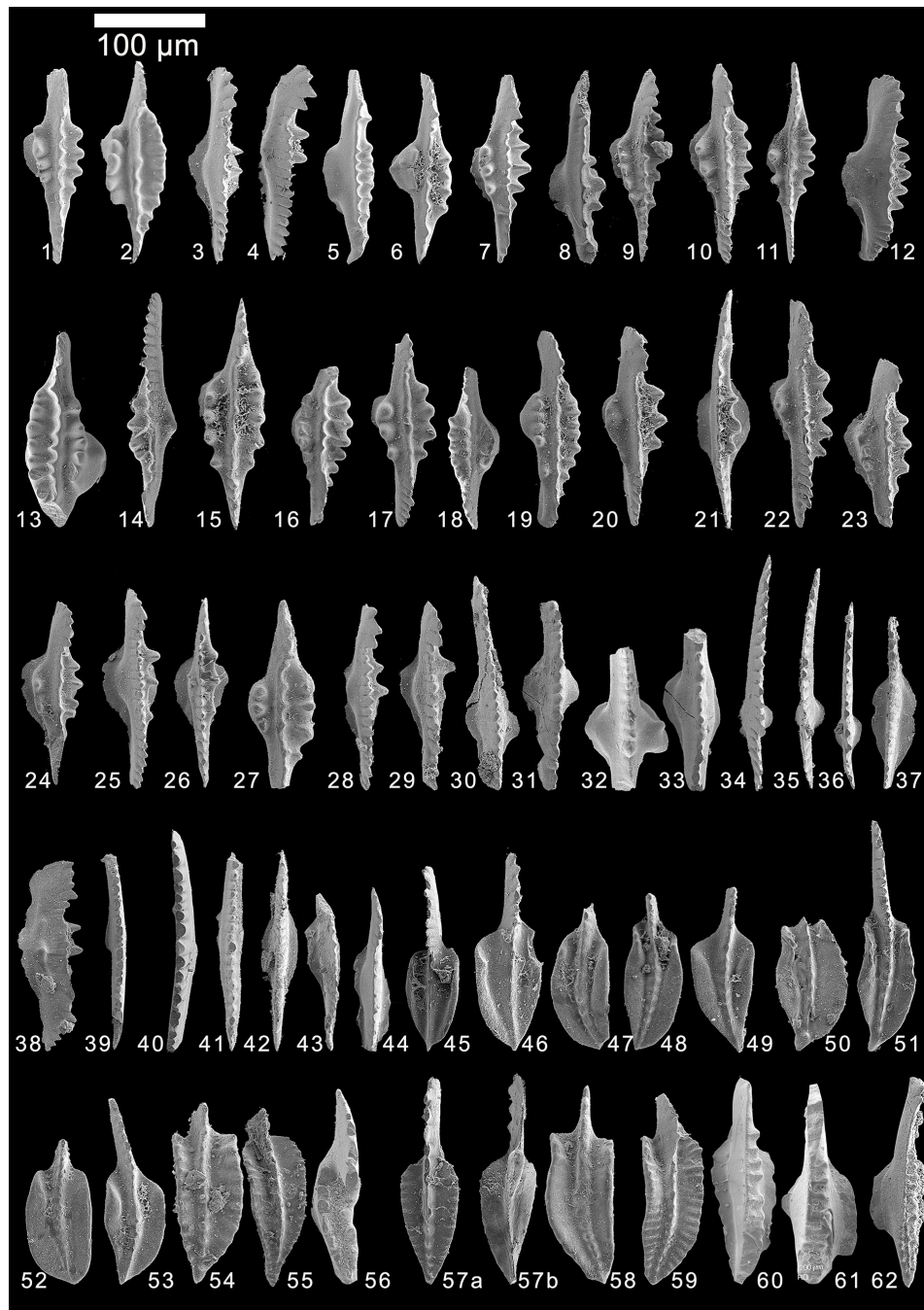


Figure 5 Conodonts from the Tuye-Darvar section, the scale bar is 100 μ m. 1, 7, 10, 11, 15, 22, 23, 24- *Pseudopolygnathus multistriatus* Branson and Mehl, 1934b; 2, 6, 16, 17, 18, 19, 27- *Pseudopolygnathus primus* Branson and Mehl, 1934; 3, 20, 21, 25, 26, 28, 29- *Bispathodus aculeatus aculeatus* Branson and Mehl, 1934a; 4, 14, 38- *Bispathodus aculeatus plumulus* (Rhodes et al., 1969); 5- *Bispathodus spinolicostatus* Branson, 1934; 8, 12, 14- *Bispathodus aculeatus aculeatus* Branson and Mehl, 1934a; 9- *Pseudopolygnathus dentilineatus* Branson, 1934; 13- *Clydagnathus plumulus* (Rhodes et al., 1969); 30, 31, 33- *Bispathodus stabilis vulgaris* (Dzik, 2006) [M1]; 32- *Bispathodus stabilis bituberculatus* (Dzik, 2006) [M3]; 34, 35, 36- *Branmehla inornata* (Branson and Mehl, 1934a); 37- *Bispathodus stabilis stabilis* (Branson and Mehl, 1934a) [M2]; 39, 40, 41, 42, 43- *Bispathodus stabilis vulgaris* (Dzik, 2006) [M1]; 44- *Bispathodus bispathodus* Ziegler et al., 1974; 45, 46- *Polygnathus communis communis* Branson and Mehl, 1934b; 47-53- *Polygnathus communis dentatus* Druce 1969; 54- *Polygnathus inornatus* Branson, 1934; 55- *Polygnathus semicostatus* Branson and Mehl, 1934; 56- *Scaphignathus velifer velifer* Helms, 1959; 57- *Polygnathus delicatulus* Ulrich and Bassler, 1926; 58- *Polygnathus padovanii* Perri and Spalletta 1990; 59- *Polygnathus inornatus inornatus* Branson, 1934; 60, 61- *Bispathodus jugosus* (Branson and Mehl, 1934a); 62- *Bispathodus ultimus* M1 Bischoff, 1957. For more details, see Appendix 1.

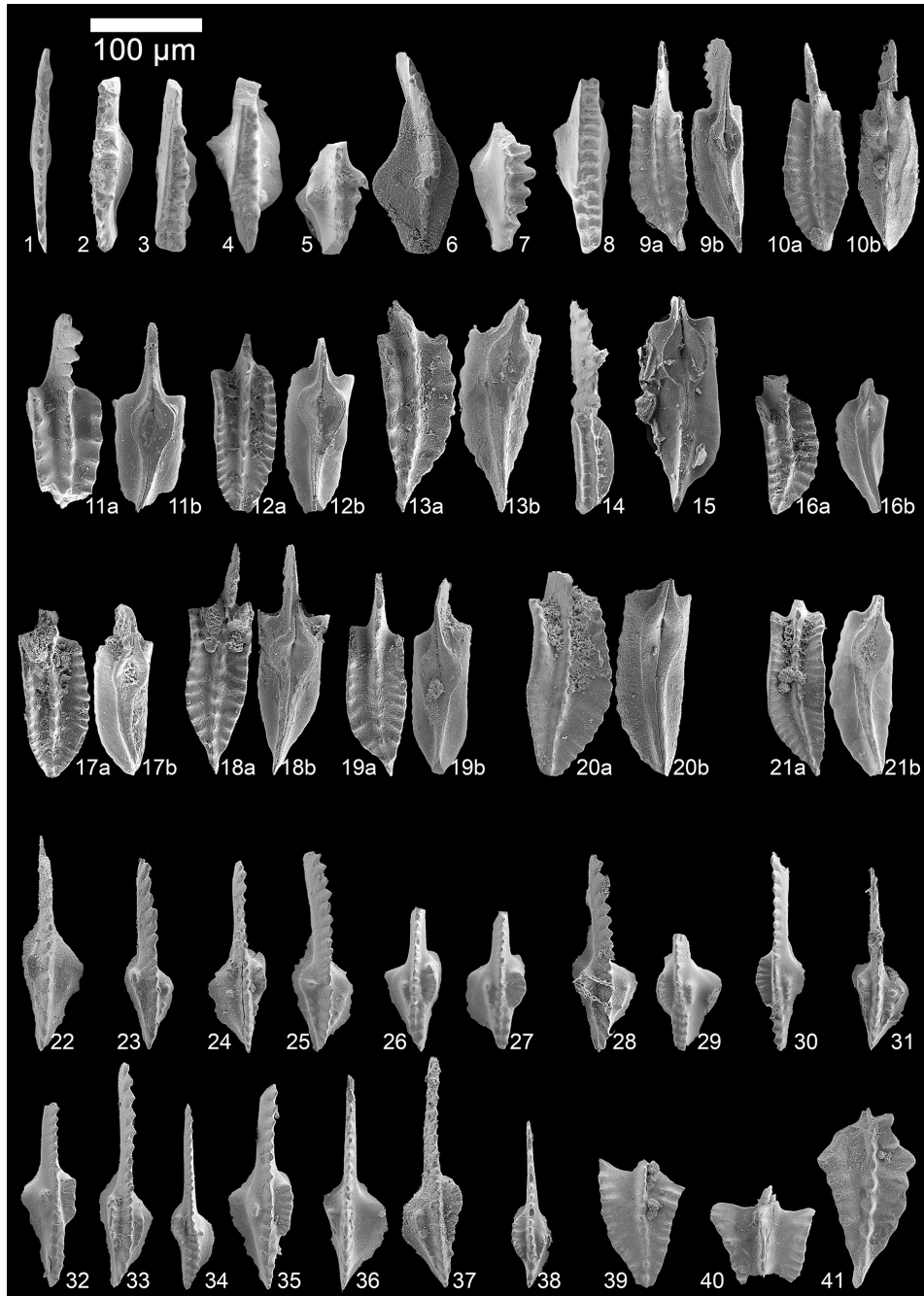


Figure 6 Conodonts from the Tuye-Darvar section, the scale bar is 100 μm . 1- *Bispathodus stabilis vulgaris* (Dzik, 2006) [M1]; 2- *Bispathodus bispathodus* Ziegler et al., 1974; 3- *Bispathodus costatus* (Branson 1934) Morphotype 2; 4, 8- *Bispathodus jugosus* (Branson and Mehl 1934a); 5- *Bispathodus aculeatus aculeatus* Branson and Mehl, 1934a; 6- *Palmatolepis minuta minuta* Branson and Mehl 1934a; 7- *Bispathodus aculeatus aculeatus* Branson and Mehl, 1934a; 9, 10, 20- *Polygnathus inornatus* Rhodes et al., 1969; 11, 12, 15, 17- *Siphonodella praesulcata* M2 Sandberg, 1972; 13, 16, 19- *Siphonodella sulcata* Huddle, 1934; 14- *Polygnathus communis communis* Branson and Mehl, 1934b; 26, 27, 29, 30, 32, 35- *Gnathodus pseudosemiglaber* Thompson and Fellow, 1970; 31, 37- *Gnathodus cueneiformis* Mehl and Thomas, 1974; 33, 38- *Gnathodus typicus* Cooper, 1939; 39, 40, 41- *Pseudopolygnathus* cf. *oxypageus* Lane et al., 1980; 24, 34, 36- *Gnathodus semiglaber* Bischoff, 1957; 18, 21- *Polygnathus longiposticus* Branson and Mehl, 1934; 23, 25- *Protognathodus collinsoni* Ziegler, 1969; 28- *Protognathodus kockeli* (Bischoff, 1957); 22- *Protognathodus meischneri* Ziegler, 1969. For more details, see Appendix 2.

5.12. SCALIKNATHUS ANCHORALIS-DOLIOGNATHUS LATUS ZONE

This Zone is defined by *Scaliognathus anchoralis* Lane and Ziegler 1983 and *Doliognathus latus* Branson and Mehl, 1941 [M2], both have their first occurrences in the *Scaliognathus anchoralis-Doliognathus latus* Zone but they are absent in Tuye-Darvar section. According to studies Lane *et al.* (1980), the first occurrence of *Gnathodus pseudosemiglaber* Thompson and Fellows, 1970, which ranges from *anchoralis-latus* Zone to *texasus* Zone at Sample S36 indicate *Scaliognathus anchoralis-Doliognathus latus* Zone. *Gnathodus semiglaber*, *Pseudopolygnathus oxypageus* occur in this sample.

6. Sedimentology and facies analysis

6.1. SEDIMENTOLOGY OF SILICICLASTIC ROCKS

Siliciclast facies settings of the Tuye-Darvar section are summarized in Table 2 (see also Figures 7, 8 and 9).

6.2. MICROFACIES

Based on carbonate microfacies studies, seven microfacies were distinguished which belong to three facies environments of tidal environment, barrier, and open marine. Non-skeletal components

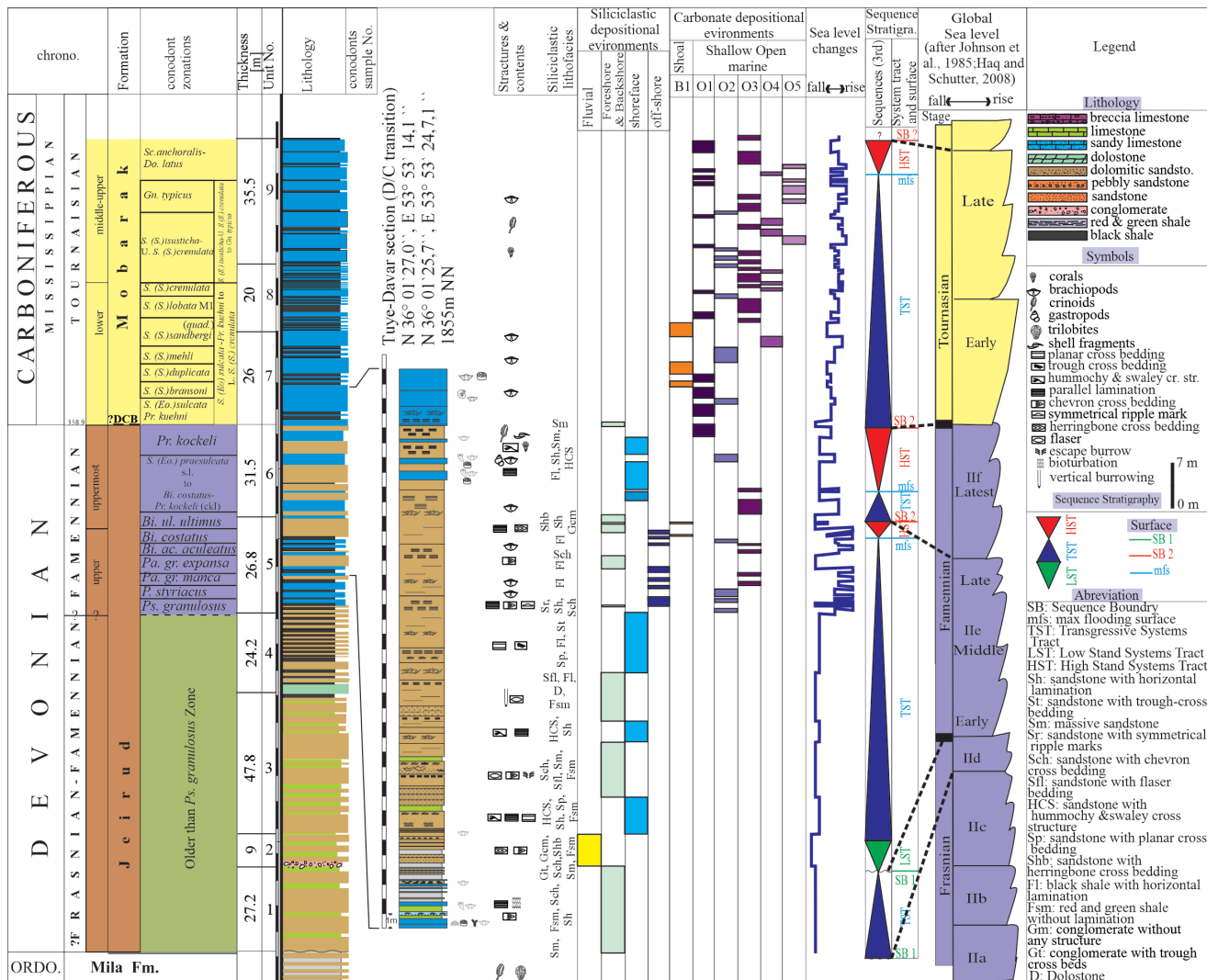


Figure 7 Distribution columns of pertofacies and microfacies, depositional environments, sea level changes, and the third-order sequences in the Tuye-Darvar Section and they are compared with third-order sequences nomenclature of Johnson *et al.*, 1985 (after Johnson *et al.*, 1985; Haq and Schutter, 2008).



Figure 8 (a) The presence of a conglomerate layer with trough cross-bedding between two massive clast-supported conglomerate layers, (b) A microscopic image of the polygenetic conglomerate (Gcm), (c) The presence of fining-upward cycle in Gt lithofacies, (d) A microscopic image of the polygenetic conglomerate (Gt), (e) Massive sandstone (Sm), (f) a microscopic image of quartz arenite petrofacies (Sm), (g) and (h) Sandstone with parallel lamination (Sh), (i) A microscopic image of fine quartz arenite petrofacies (Sh), (j) Sandstone layer, showing chevron cross-bedding (Sch), (k) A microscopic image of medium- to coarse-grained quartz arenite petrofacies (Sch), (l) Sandstone layer, indicating herringbone cross-stratification (Shb), (m) A microscopic image of medium-grained quartz arenite petrofacies (Shb), (n) Sandstone layer, showing planar cross-stratification (Sp), (o) A microscopic image of medium-grained quartz arenite petrofacies (Sp).

included peloids, intraclasts, cortoids, while skeletal constituents involved benthic foraminifera, brachiopods, mollusks, gastropods, cephalopods, bryozoans, calcispheres, echinoderms, and sponges, which are summarized in Table 3 (Figures 7 and 10).

6.3. SEDIMENTARY ENVIRONMENT

According to our sedimentary/facies studies, four depositional facies setting at mixed carbonate-siliciclastic platform were identified (Figure 11):

6.3.1. FLUVIAL ENVIRONMENT FACIES ASSOCIATION

This association including Gcm, Gt, Sm, Sch, Shb and Fsm, and contains conglomerates, sandstones, and red mudrocks. The beginning of this association is marked by presence of clast-supported massive polygenetic conglomerate (Gcm) on both sides of the conglomerate layer with fining-upward cycles and trough crossbedding indicating channel geometry. Later on turning into the red massive gravelly sandstone without define structure, showing very poorly sorted texture, after that to the massive coarse- to medium-grained sandstone (Sm). The complex contains hematite cement, which indicates the deposition of the sediments in a non-marine and fluvial environment (Omali *et al.*, 2011). The flood plain sediments include red mudrocks without any lamination (Fsm). During the field observation and laboratory studies no fossils were found from these mudrocks. All of the above shows these deposits can be attributed to the oxidized mudstones of the flood plain (Lewin and Ashworth, 2014; Sharafi *et al.*, 2016). The tidal-influenced river channel represents the presence of arkosic sands with a medium sorting, medium grain-size, and angular-semirounded grains, - these channels indicate the maximum tidal limit toward the lands (Ichaso and Dalrymple, 2006), among which some have no structure (Sm) and some show herringbone (Shb) and chevron (Sch) cross-bedding structures. These structures are formed in the rivers influenced by marine tides (Longhitano *et al.*, 2012; Sharafi *et al.*, 2016). The abundance

of coarse-grained sediments and the remarkable thickness of intra-channel deposits, compared with the flood plain deposits (fine-grained), indicate the presence of shallow channels with low sinuosity, low base level, high sediment supply, and low accommodation space; as a result, this river is a braided one with sandstone-conglomerate bed load (Miall, 2006; Foix *et al.*, 2013) (Figure 12). As well, this type of river has been reported from the Tuye-Darvar section by Sharafi *et al.* (2014).

6.3.2. FACIES ASSOCIATION OF WAVE-DOMINATED FORESHORE AND BACKSHORE PARTS

This association consists of an alternation of thick-bedded sandstones and thin-bedded shales, including Sh, Sm, Sfl, Sr, Fsm, Fl, Gcm, Sp, Sch, Shb and D facies (Miall, 2006; Dumas and Arnott, 2006; Bayet-Goll *et al.*, 2016; Sharafi *et al.*, 2016). The association includes sands with quartz arenite to sub-litharenite facies; the grain size is medium to large; they are medium- to well-sorted and medium to well-rounded, and the cement between the grains is occasionally dolomitic. The allochemical sandstones whose formation is related to the tidal environment, are frequently found in this association (Ghorbani *et al.*, 2014; Sharafi *et al.*, 2016). The bioturbation and fossil traces sporadically include vertical to oblique burrows. The presence of green mudrocks, which have no laminations and trace fossils (Fsm), indicates sedimentation from suspension in a low-energy environment (Reineck and Singh, 1980; Sharafi *et al.*, 2016). The vertical burrow traces are specific to shoreface and barrier environments with high-energy (Uchman and Krenmayr, 2004; Sharafi *et al.*, 2016). The lithofacies Sfl represents the tidal flat (Bhattacharyya and Chakraborty, 2000; Ghosh *et al.*, 2006; Khalifa and Catuneanu, 2008). The facies Sr formed in low flow regimes, shallow water, influenced by the ripples motion and fine particle deposition in tidal cycles (Harms *et al.*, 1982; Reineck and Singh, 1980). These ripples are the result of reciprocating flow that relates to the tidal flats to the coastal environment (Zand-Moghaddam *et al.*, 2014). In addition to

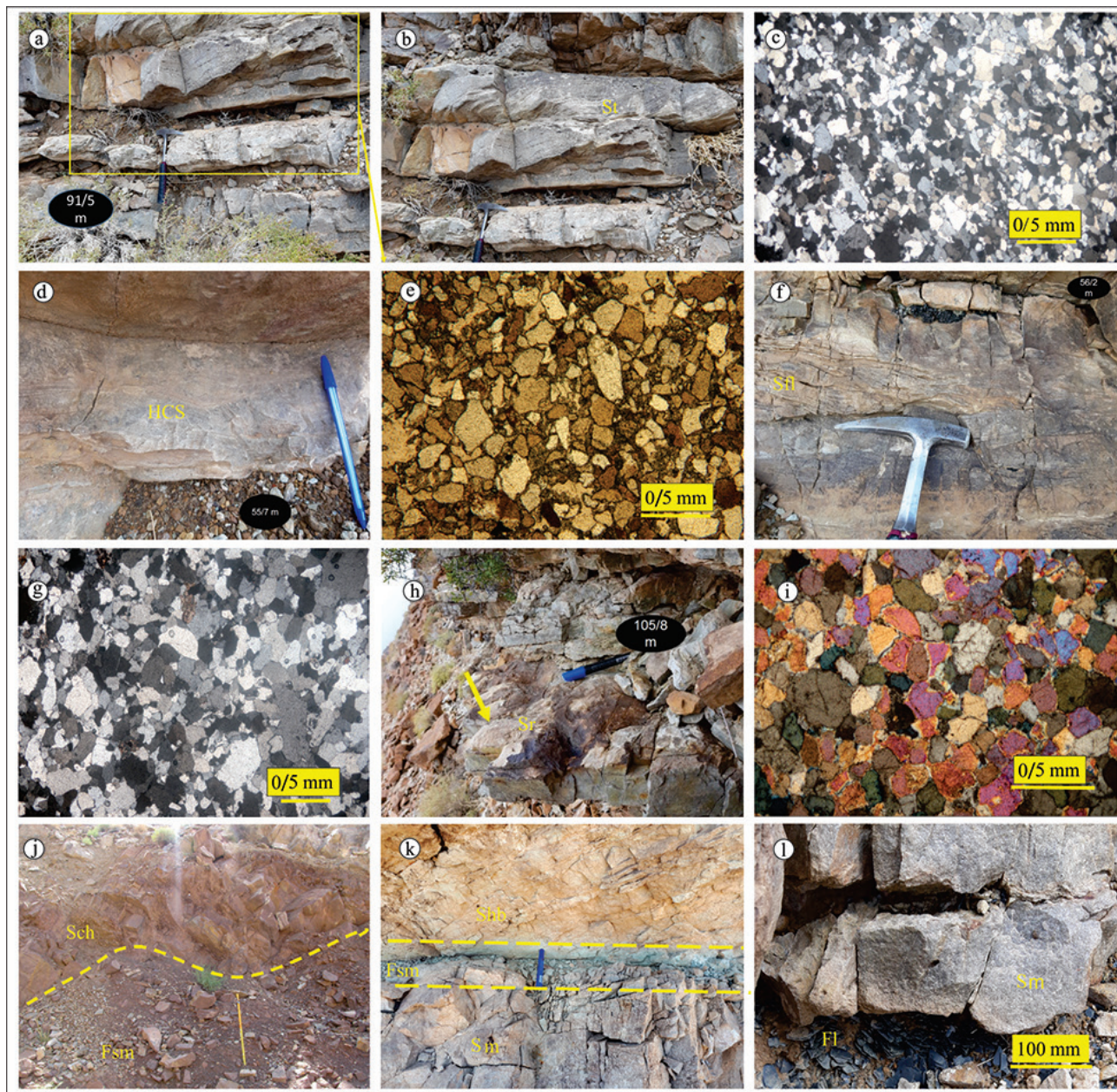


Figure 9 (a), (b) Sandstone layer, showing trough cross-bedding (St), (c) A microscopic image of medium-grained quartz arenite petrofacies (St), (d) Sandstone layer, showing hummocky cross-stratification (HCS), (e) A microscopic image of quartz arenite petrofacies (HCS), (f) Sandstone layer, showing flaser structure (Sfl), (g) A microscopic image of medium-grained quartz arenite petrofacies (Sfl), (h) Sandstone layer, showing symmetrical ripple mark (Sr), (i) A microscopic image of medium-grained quartz arenite petrofacies (Sr), (j) Red mudrocks facies (Fsm), (k) Green mudrocks facies (Fsm), (l) Dark laminated mudrocks facies (Fl).

Table 2. Lithofacies.

Facies	Lithology	Sorting	Size	Features
Gcm: conglomerate without any structure (massive)	White microconglomerate and red conglomerate	Very poorly sorted	Silt-size to 5 cm	Different fragments (chert fragments, igneous rocks, sandstones, clay, and fossil fragments) containing intergranular space or medium-grained filled sandstone
Gt: conglomerate with trough cross-beddings	red conglomerate	Poorly sorted	Silt-size to 8 cm	Trough cross-bedding (about 10-degree dip), including volcanic fragments, siltstone, and sandstone
Sm: massive sandstone	White, brown, red, and yellow sandstones	Moderately to well sorted	Fine-grained to medium-grained	Without any structure or bedding, showing quartz arenite, allochemical sandstone, and dolomitic sandstone petrofacies, with the sporadic fossils
Sh: sandstone with horizontal lamination	White and brown-yellow sandstones	Moderately to well sorted	Very fine-grained to medium-grained	Parallel lamination, some parts of this lithofacies in the alternation with clay facies are more fine-grained.
Sch: sandstone with chevron cross-bedding	White and red sandstones, and buff to brown dolomitic sandstones	Relatively well sorted	Medium-grained	Chevron cross-bedding
Shb: sandstone with herringbone cross-bedding	red sandstones	Relatively well sorted	Fine-grained to medium-grained	Herringbone structure (a structure that the upper and lower laminations have a difference of 180 degrees)
Sp: sandstone with planar cross-bedding	White quartz arenites	Well to moderately sorted	Medium-grained	Planar cross-bedding with an angle of 20-25 degrees.
St: sandstone with trough cross-bedding	White quartz arenites	Relatively well sorted	Medium-grained	Trough cross-bedding
HCS: sandstone with hummocky and swaley cross stratification	White and gray sandstones	Poorly sorted	Various grain size	Hummocky cross-stratification, including trace fossils and bioturbation
Sfl: sandstone with flaser bedding	White quartz arenites	Moderately sorted	Medium-grained	Flaser structure and vertical to oblique burrow
Sr: sandstone with symmetrical ripple marks	White quartz arenites	Very well sorted	Medium-grained to coarse-grained	Symmetrical ripples with a thickness of 8-10 cm
Fsm: red and green shale without lamination	Red and green mudrocks	-	Fine-grained mud particles (silt and clay)	Non-laminated and without fossils; in contact with Sm, Shb, Sch, Sm, Sfl, HCS, and Gm
Fl: black shale with horizontal lamination	Dark mudrocks	-	Fine-grained mud particles (silt and clay)	Laminated (due to the abundance of clay minerals), showing flat levels parallel to bedding surface; with sporadic presence of brachiopods; in contact with Sm, Sr, St, Sp, Sch, and Shb facies

one-directional flows, facies Sp formed in two-directional flows (including coastal reciprocating flows) (Tucker, 2001). Sch and Shb lithofacies can also be deposited in environments with reciprocating and fluctuating flows such as tidal flats (Reineck and Singh, 1980; Strand, 2005). The facies Gm can be considered as a conglomerate, resulting from the destructive action of waves on the foreshore (Catuneanu *et al.*, 2003), and immediately on it, there is a transgression on the foreshore and the deposition of deeper facies of shoreface. The presence of sandy dolostones (D) and their alternation with mudrocks (Fl) indicate that these dolostones are deposited primarily (Adabi and Mehmandosti, 2008; Chen *et al.*, 2010). Besides, the formation of dolomite is because of the high amounts of magnesium and its high ratio to the calcium content in the water inside the cavities (Flügel, 2010). The presence of dolomite in tidal environments with high water fluctuations is usual (Zonneveld *et al.*, 2001; Chen *et al.*, 2010) (Figure 13).

6.3.3. FACIES ASSOCIATION OF UPPER AND LOWER SHOREFACE

This association includes Sh, HCS, St, Sm, Fl, Fsm facies, and deposited in the lower and upper shoreface (Dumas and Arnott, 2006; Bayet-Goll *et al.*, 2016; Sharafi *et al.*, 2016). The facies type is quartz-arenite to sub-arkose with dolomite and silica cement. The size of the sand grains is moderately sorted fine to occasionally medium. The presence of cross-bedding and rounded quartz grains indicates a high-energy coastal environment, related to the upper sub-environment of the foreshore (Chakraborty and Sensarma, 2008). Trough cross-bedding in sandstones (St) is the wave performance (Moslow and Tye, 1985). Sandstones with parallel lamination (Sh) are also able to form in the outer flat zone of the upper shoreface (Einsele, 2000). The lack of fossil remains in these facies can be due to the high prevailing energy in the sedimentary environment and as a result of stressful living conditions for organisms (Selle, 2000). The lithofacies Sm is the result

of rapid deposition of sand grains after storm currents (Sharafi *et al.*, 2016) (Figure 16). Quartz arenite to sub-litharenite facies, medium to well sorting, roundness, and facies association of Sh, Sm, Sfl, Sr, Fsm, Fl, Gcm, Sp, Sch, Shb, and D, all indicate the deposition of this association in wave-dominated foreshore and backshore sub-environments (Figure 14).

6.3.4. OFFSHORE FACIES ASSOCIATION

The distribution of this association is related to the upper parts of the Jeirud Formation and includes facies Fl of dark laminated mudrocks. The facies (Fl) formed due to calm conditions and inactivity of organisms; these facies shaped in a storm-influenced shelf environment, in the post-storm quietness below wave base (Reineck and Singh, 1980; Tucker and Wright, 1990; Vakarelov *et al.*, 2012). The facies is deposited in the lower offshore and mostly at low energy water flow and as a result of suspended flows and calm conditions; it forms a considerable thickness of mudrock facies (Miall, 2006; Higgs *et al.*, 2012). The dark color of these mudrocks indicates their precipitation in relatively deep and reduction conditions as well as weak drainage (Mack and James, 1992; Flügel, 2010) (Figure 15).

6.3.5. OPEN MARINE FACIES ASSOCIATION

The deposits of the Jeirud Formation start with the siliciclastic sediments of the wave-dominated foreshore and backshore environment; there are red fluvial (braided) continental deposits on it, and then up to the Devonian-Carboniferous boundary (DCB), the wave-influenced deposits of lower and upper shoreface, and foreshore and backshore parts are alternately repeated. Over in the section there are deposits, related to the deep offshore and carbonate deposits alternately, and then all four mentioned environments alternately deposited by sea-water progradation and retrogradation, siliciclastic sediments entry or lack of them. The Carbonate sediments have

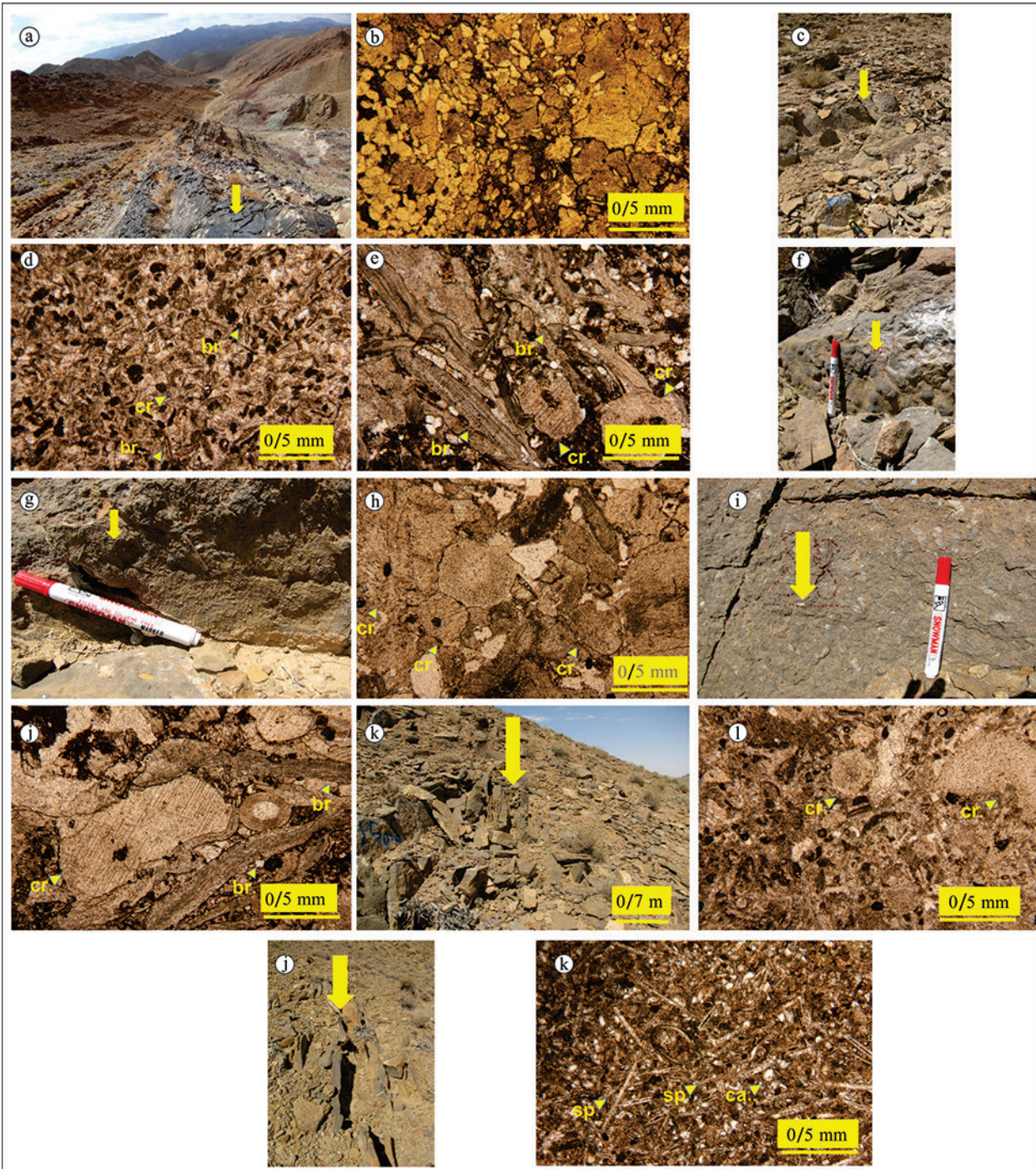


Figure 10 (a) Brown dolomite, (b) Sandy Dolostone (D), (c) Medium-bedded gray limestone containing crinoids and brachiopods, (d) Pelloid bioclast brachiopod crinoid packstone (B), (e) Sandy bioclast rudstone (O1), (f) Medium-bedded gray limestone, containing brachiopods, (g) Medium-bedded gray limestone, containing crinoid fragments, (h) Bioclast crinoid grainstone (O2), (i) Light gray limestone containing brachiopods and coarse crinoids, (g) Bioclast brachiopod crinoid rudstone, (O3), (k) Medium-bedded gray limestone, (l) Pelloid bioclast crinoid packstone (O4), (m) Thin- to medium-bedded dark gray limestone, (n) Spiculite calcisphere bioclast packstone (O5).

Table 3. Carbonate microfacies.

Microfacies	Lithology	Major components	Minor components	Features
D: sandy dolostone	Brown dolomites (the Jeirud Formation)	Dolomite + Sand (about 18%)	-	In alternation with (F1); probably, dolomites are primary, formed as sea level falls, and are related to tidal environments with high fluctuations (Zonneveld <i>et al.</i> , 2001; Chen <i>et al.</i> , 2010)
B: pelloid bioclast brachiopod crinoid packstone-grainstone	Medium-bedded to thick-bedded gray sandy limestone, including brachiopods and crinoids (the Jeirud and Mobarak formations)	Peloids, brachiopods, and crinoids	Bryozoans, gastropods, ostracods, <i>Earlandia</i>	Low diversity of fossils, grains well sorting and grain-supported texture and wide spatial distribution of crinoids indicate the high water activity and the presence of these microfacies above the wave base. All evidence shows the deposition of the microfacies in the bioclastic barrier sub-environment (Flügel, 2010; Ahmed <i>et al.</i> , 2006).
O1: sandy bioclast packstone-grainstone-floatstone-rudstone	Medium-bedded to thick-bedded gray sandy limestone, including brachiopods and crinoids (the Jeirud and Mobarak formations)	Brachiopods, crinoids, quartz grains	Bryozoans, gastropods, ostracods, bivalves, peloids, corals	Due to the presence of a high amount of quartz grains and lack or deficiency of micrites, these microfacies should be formed in a high energy environment (Shinn, 1983, 1986). The fall of relative sea-level leads to the transfer of backshore sands, and the entry of continental sands indicates the development of a bioclastic barrier near the shoreface (Armella <i>et al.</i> , 2007).
O2: bioclast crinoid packstone-grainstone	Medium-bedded to thick-bedded gray limestone, including brachiopods and crinoids (the Jeirud and Mobarak formations)	Crinoids	Gastropods, bivalves, peloids, mud intraclasts, <i>Earlandia</i> , ostracods	Poorly sorted compare to the bioclastic barrier microfacies, the presence of crinoids and grain-supported texture indicate low energy, shallow depth, and deposition in open marine slope toward the barrier environment (Flügel, 2010).
O3: bioclast brachiopod crinoid floatstone-rudstone	Medium-bedded to thick-bedded gray limestone, including brachiopods and crinoids (the Jeirud and Mobarak formations)	Brachiopods, crinoids	Bryozoans, gastropods, bivalves	Severe development of cortoids – carbonates of shallow marine shelves and carbonate platforms are appropriate for the formation of cortoids (Flügel, 2010) – these microfacies are deposited in a low energy environment of an open marine slope, near the sea wave-base in a normal condition (Machel and Hunter, 1994) and formed in a moderate to high wave energy near the wave-base (Flügel, 2010).
O4: pelloid bioclast crinoid packstone-grainstone	thin-bedded to medium-bedded gray sandy limestone, including corals and crinoids (the Mobarak Formation)	Crinoids, peloids	Brachiopods, ostracods, quartz grains (about 5%)	In these microfacies, the grains are poorly to moderately sorted; given the stratigraphic position, abundant crinoids, and the presence of peloids as well as grain-supported texture, the formation of these microfacies can be attributed to the open marine below the wave base (Hüneke, 2001; Colombié and Strasser, 2005).
O5: spiculite calcisphere bioclast wackestone-packstone	thin-bedded to medium-bedded dark gray limestones, (the Mobarak Formation)	Spicules, calcispheres	Crinoids, gastropods, ostracods, quartz grains (about 5%)	The presence of spicules and calcispheres confirms the deposition of these microfacies in a deep and semi-deep marine environment with low hydrodynamic energy below fair-weather wave base (Flügel, 2010). In some thin sections, there are about 5 percent quartz grains (their presence stems from lack of continuous bioclastic barriers) (Armella <i>et al.</i> , 2007).

been extensively presented after the Devonian/Carboniferous Boundary (DCB). The siliciclastic deposits, especially of the Devonian period related to the Jeirud Formation, form a large thickness of the studied profile, so that the entry of siliciclastics into the basin with a large volume, has not allowed organisms to flourish and form a complete carbonate ramp, including inner, middle and outer ramp. The carbonate platform in the Carboniferous Mobarak Formation has been formed due to the low entry of siliciclastics and the deposition of carbonate sediments. The absence of interconnected reef barriers, the presence of bioclastic shoal, lack of collapsing and slippery sediments, and the gradual facies change relative to each other indicate two sub-environments including the inner ramp (the only facies in the inner ramp is bioclastic facies (B1: Pelloid bioclast brachiopod crinoid packstone grainstone) and middle ramp (containing O1 to O5 microfacies).

7. Sequence stratigraphy

The sequence stratigraphy studies the sequences that are genetically related to each other and bounded between two sequence boundaries (unconformities or their correlative conformities) (Catuneanu *et al.*, 2005, 2009). Sea level changes lead to the vertical accumulation of facies, which indicates sequence stratigraphy (Catuneanu *et al.*, 2003). In other words, the history of sedimentation, erosion, and sea-level changes in an area is determined by sequence stratigraphic studies. In this research, different parts of each sequence were distinguished based on models presented by Hunt and Tucker (1992), Emery and Myers (1996) and Catuneanu *et al.* (2003). According to the mentioned references, there are four sedimentary tracts, including lowstand systems tracts (LST), transgressive systems tracts (TST), highstand systems tracts (HST) and forced regressive systems tracts (FRST). Based on the available evidence of field observation and laboratory studies, especially facies showing the Maximum Flooding

Surface (mfs) and lowest water level, 3 third-order complete sequences and 1 incomplete sequence were detected, consisting of three sedimentary tracts of LST, TST, and HST (Figure 7).

7.1. SEQUENCE 1

This sequence encompasses 27.5 m of the section from the base (Unit 1 of the Jeirud Formation with the Late Devonian in age); this sequence is incomplete and only includes TST, bounded between two boundaries of type I. The sequence boundary at the base of the studied section is equivalent to a disconformity so that due to the Caledonian epirogenic event, there are not the Silurian, the Lower to Middle Devonian, and part of the Upper Devonian sediments; and the Upper Devonian quartz arenite sands cover the Ordovician green shales. Because of the presence of non-marine (fluvial) deposits on the marine deposits, the upper boundary of this sequence is of type I. The deposits present in the Sequence 1 include sandstone sediments with Sm, Sh, and Sch facies, and red and green non-laminated mudrocks (Fsm) that are related to the wave-dominated foreshore and backshore environment; the shale content increases upward. This sequence is corrolatable with the last Frasnian sequence that recognized by Johnson *et al.* (1985) (IId) (Figure 7).

7.2. SEQUENCE 2

This sequence (107.5 m), which is situated on sequence 1 is the Late Devonian in age (units 2, 3, 4, and 5 of the Jeirud Formation), and consists of LST, TST, and HST. It is characterized by a decrease in water-level and the presence of fluvial facies (LST) on sequence 1. This sedimentary systems tract with Gcm, Gt, Sm, Sch, Fsm, and Shb facies is 10.3 m thick. On this sedimentary systems tract, there is an increase in sea-level as TST (91.2 m) and includes wave-dominated foreshore and backshore, lower and upper shoreface environments, B1, O2, O3, and offshore

microfacies. In this sequence, mfs is dark laminated mudrocks (F1) of the offshore environment. The highstand systems tract (HST) (6 m) in the sequence includes microfacies B1 in the inner ramp and wave-dominated foreshore and backshore parts. The sequence boundary is characterized by the presence of a thin layer of microconglomerate, which is the shallowest facies of this sequence and according to the lack of any evidence of exposure from water, this sequence boundary is of type

II. This sequence is corrolatable with the first Famennian sequence that recognized by Johnson *et al.* (1985) (IIe) (Figure 7).

7.3. SEQUENCE 3

This sequence (31 m) consists of two sedimentary systems tracts of TST and HST (Unit 6 of the Jeirud Formation, related to the Late Devonian), containing quartz arenite sandstones (sands belonging to the wave-dominated foreshore and

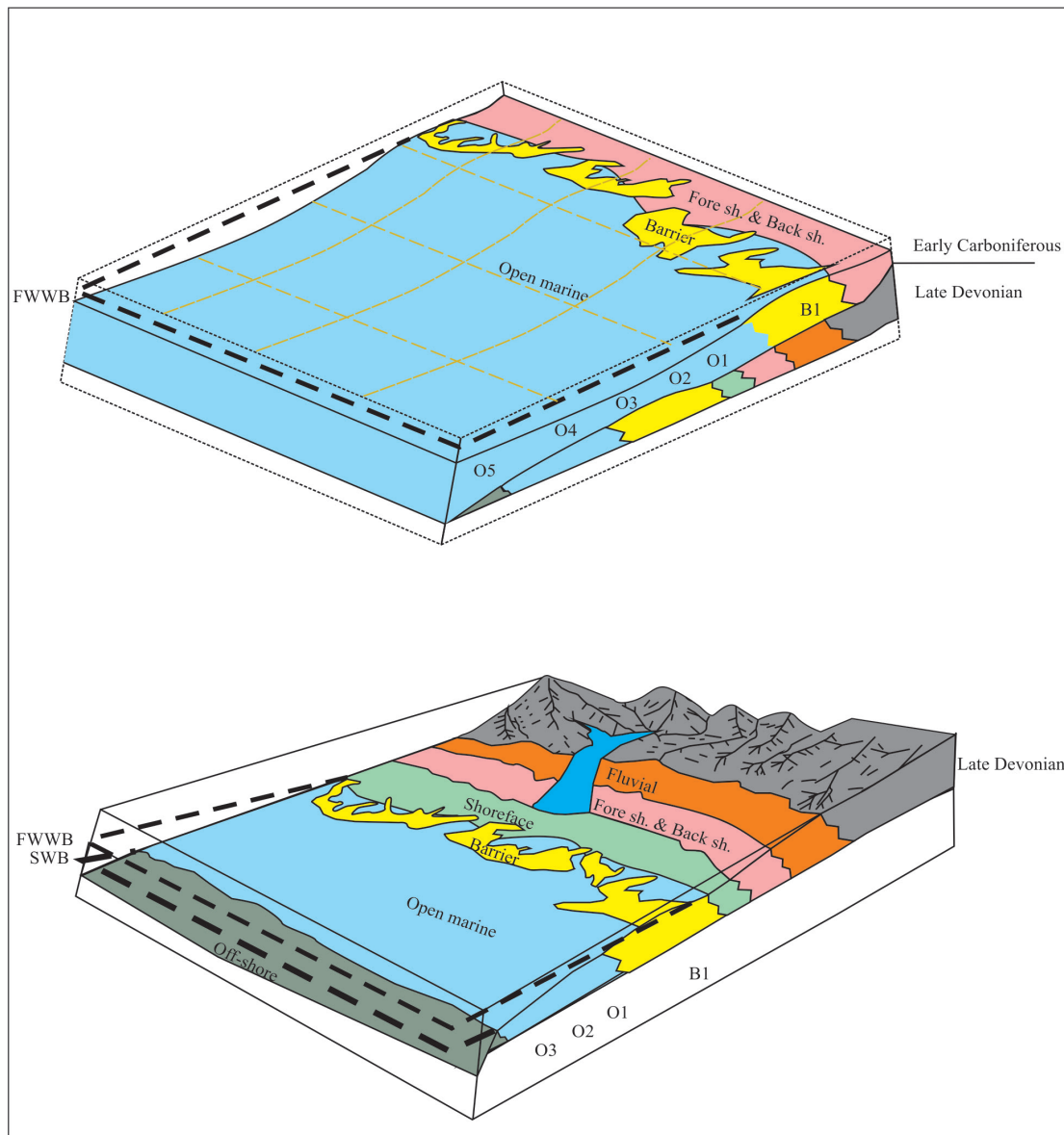


Figure 11 Sedimentary environment of the Tuye-Darvar Section based on the existing facies.

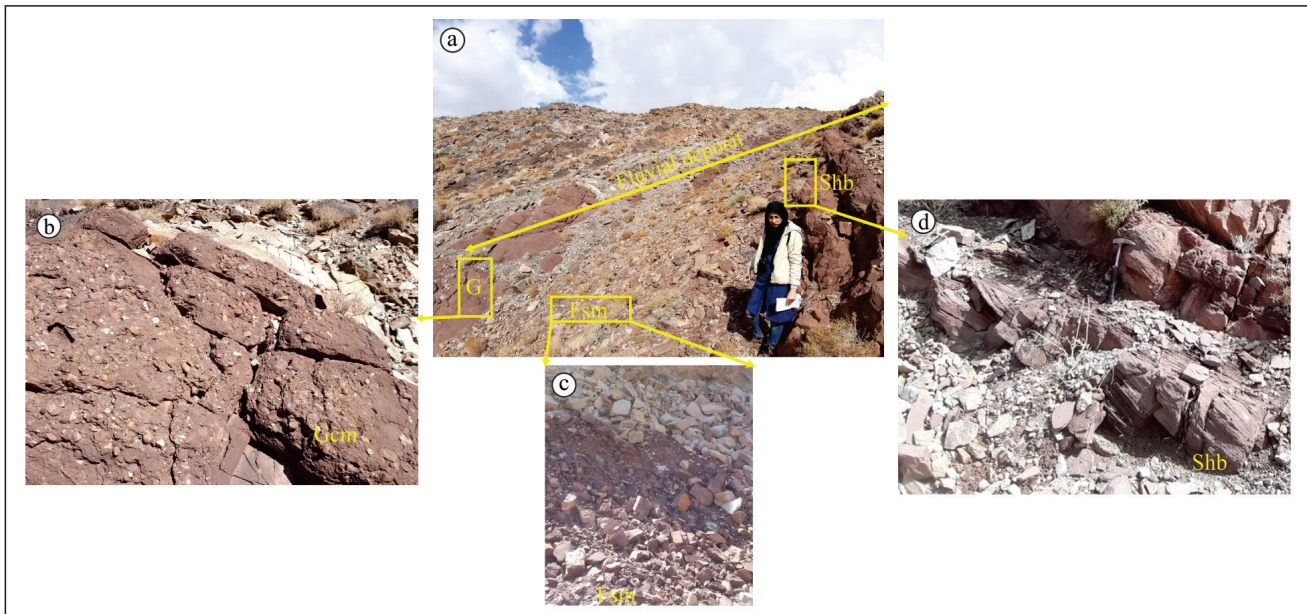


Figure 12 (a) Fluvial facies association of the studied section, (b) Clast-supported massive conglomerate (Gcm), (c) Non-laminated red mudrock (Fsm), (d) The sandstone showing herringbone cross-bedding (Shb).

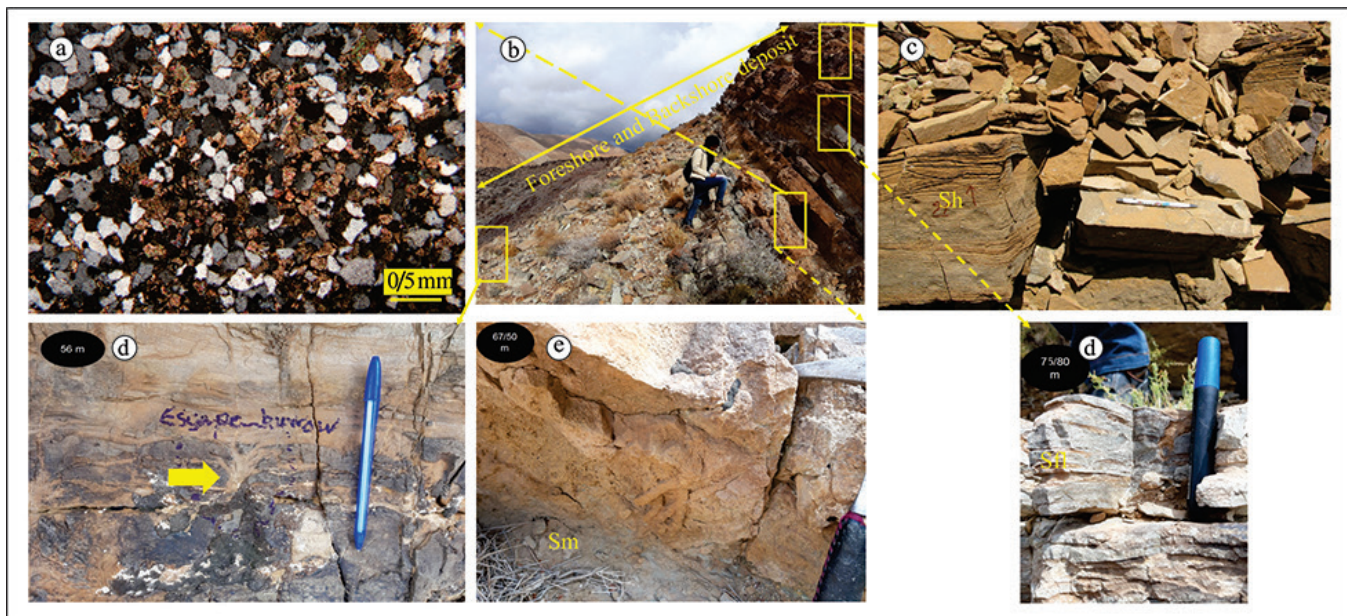


Figure 13 Facies association of wave-dominated foreshore and backshore parts: (a) Allochemical sandstone, (b) Part of the wave-dominated foreshore and backshore deposits, (c) Sandstone with parallel lamination, (d) Sandstone with escape burrows, (e) Massive sandstone with vertical burrows (Sm), (f) Sandstone with flaser stratification (Sfl).

backshore part), fossiliferous gray limestones alternating with brown and white sands of lower and upper shoreface. The TST (9.5 m) in this sequence consists of sandstones from the lower and upper shoreface, and O3 carbonate microfacies. The deepest facies that represent mfs is O3. Then there are HST sediments (21.5 m) that include the upper and lower shoreface O2 microfacies. The upper boundary of this sequence as the shallowest facies of this systems tract is quartz arenite sandstone of wave-dominated foreshore and backshore environments; it corresponds to the DCB and is of type II. This sequence is corrolatable with the last Famennian sequence that recognized by Johnson *et al.* (1985) (III) (Figure 7).

7.4. SEQUENCE 4

This sequence (81.5 m) consists of TST and HST deposits (units 7, 8, and 9 of Mobarak Formation, related to the Early Carboniferous). The lithology of this part is dark gray limestones and laminated black shales. The TST sediments (74.5 m) in this sequence comprise B1, O1, O2, O3, O4, and O5. The mfs of this sequence is in the O5 facies as the deepest one. HST part (7 m) contains O3 and O1 microfacies, and the upper boundary of this sequence is faulted. This sequence is correlatable with the first Tournasian sequence that recognized by Johnson *et al.* (1985) (Figure 7).

8. Conclusion

DCB successions are globally characterized by conodont-free siliciclastics, stratigraphic gaps, or uncertainties among the first occurrence of biostratigraphically relevant index fossils. This resulted from regionally varying palaeoenvironmental conditions caused by global major environmental changes related to the HC. The Tuye-Darvar section yielded a succession of the biostratigraphically significant bispathodids and early siphonodellids, as well as specimens of protognathodids. The *praesulcata* and *sulcata* Zones could be well established by *Si. praesulcata* and *Si. Sulcata*, the *Prot. kockeli* Zone is also recorded. The general scarcity of the fauna can be explained by the shallow-water, high-energetic palaeoenvironment, and a relatively high siliciclastic amount in the limestones. Due to siliciclastic shallow-water deposits around the DCB the conodont fauna is scarce.

Micro-facies analysis reveals 13 siliciclastic facies (forming most of the Late Devonian sediments) as well as 7 carbonate facies (forming most of the Early Mississippian); concluded the section formed in a mixed carbonate-siliciclastic system. In the Late Devonian interval (of the Jeirud Formation), the entry of siliciclastic deposits has formed a large thickness so that the remarkable entry volume of these siliciclastics

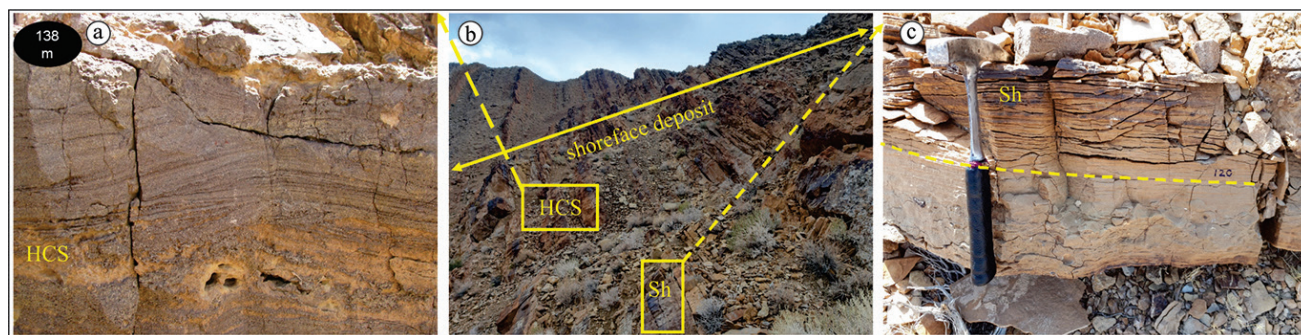


Figure 14 (a) Sandstones showing hummocky cross-stratification (HCS), (b) Upper and lower shoreface facies associations, (c) Sandstones showing parallel lamination (Sh).

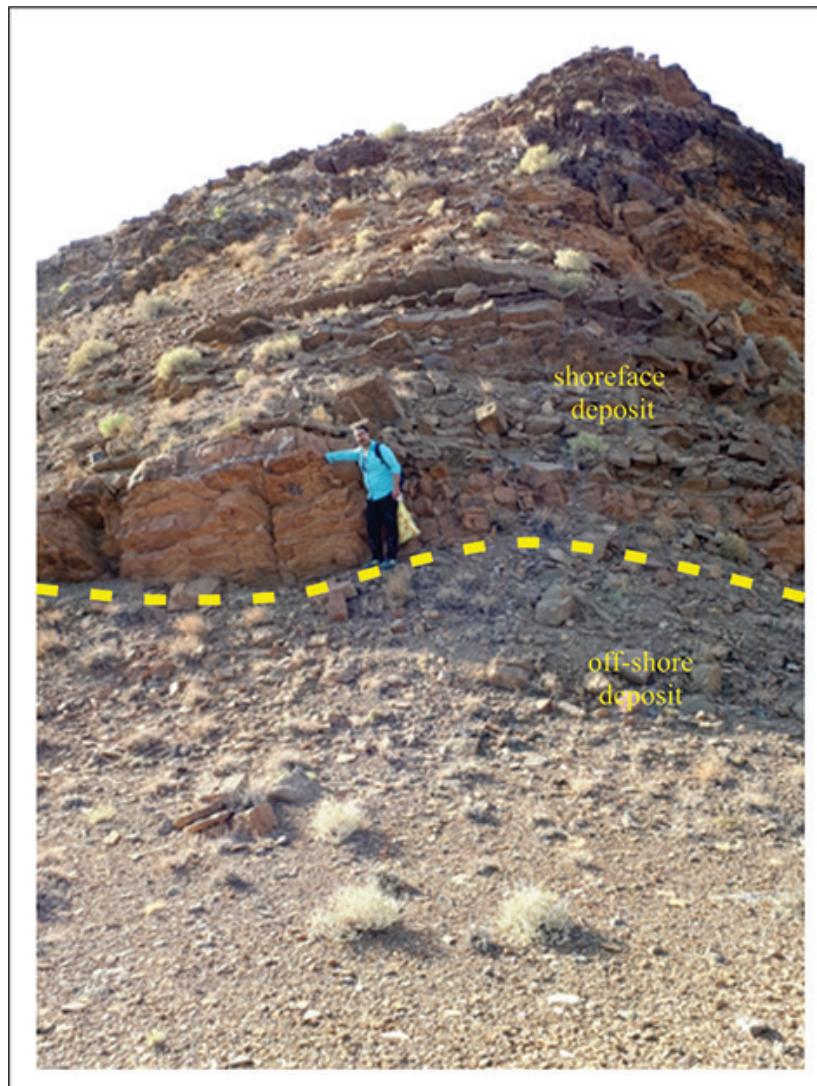


Figure 15 Offshore facies association including laminated dark mudrocks.

prevented the flourishing of organisms and formation of a complete carbonate ramp. Studying the third-order sequences in the section indicated four 3order sequence. The first three sequences belong to the Late Devonian, and the last sequence belongs to the Early Mississippian.

Conflict of interest

The authors declare that they have no conflict of interest.

Contributions of authors

Elaheh Sattari: fieldwork, basic stratigraphic data, writing part of original manuscript. Ali Bahrami: conceptualization, writing of original manuscript, figures design. Peter Königshof: Fieldwork, data interpretation, writing part of original manuscript, edition of the manuscript. Hossein Vaziri Moghaddam: partial paleontological identification and interpretation. Azizollah Taheri: fieldwork, basic stratigraphic data.

Financing

The Vice Chancellor for Research and Technology at University of Isfahan is acknowledged for financing granted to the PhD project of the first author.

Acknowledgments

Hereby, we acknowledge the Vice Chancellor for Research and Technology of the University of Isfahan. As well, the authors appreciate Department of Geology to the scientific and logistical supports.

Handling editor

Francisco J. Vega.

References

- Adabi, M.H., Mehmandosti, E.A., 2008, Microfacies geochemistry of the Ilam Formation in the Tang-E Rashid area, Izeh, S.W. Iran: *Journal of Asian Earth Sciences*, 33 (3-4), 267-277. <https://doi.org/10.1016/j.jseacs.2008.01.002>
- Ahmed, A.H.M., Bhat, G.M., Azim Khan, M.H., 2006, Depositional environments and diagenesis of the Kuldhar and Keera Dome Carbonates (Late Bathonian-Early Callovian) of Western India: *Journal of Asian Earth Sciences*, 27, 765-778. <https://doi.org/10.1016/j.jseacs.2005.06.013>
- Alavi, M., 1991, Tectonic Map of the Middle East: Geological Survey of Iran. 60 p.
- Alavi, M., 1996, Tectonostratigraphic synthesis and structural style of the alborz mountain system in Northern Iran: *Journal of Geodynamics*, 21 (1), 1-33. [https://doi.org/10.1016/0264-3707\(95\)00009-7](https://doi.org/10.1016/0264-3707(95)00009-7)
- Armella, C., Cabaleri, N., Leanza, H.A., 2007, Tidally dominated, rimmed shelf facies of the Picún Leufú Formation (Jurassic/Cretaceous boundary) in southwest Gondwana, Neuquén Basin, Argentina: *Cretaceous Research*, 28, 961-979. <https://doi.org/10.1016/j.cretres.2007.01.001>
- Aretz, M., Corradini, C., 2021, Global review of the Devonian-Carboniferous Boundary: an introduction: Palaeobiodiversity and Palaeoenvironments, 101 (4), 285-293. <https://doi.org/10.1007/s12549-021-00499-8>
- Assereto, R., 1963, The Paleozoic Foraminifera in central Elborz (Iran): Preliminary Note: *Rivista Italiana di Paleontologia e Stratigrafia*, 69, 503-543.
- Bagheri, S., Stampfli, G.M., 2008, The Anarak, Jandaq and Posht-e-Badam metamorphic complexes in central Iran: New geological data, relationships and tectonic implications: *Tectonophysics*, 451 (1-4), 123-155. <https://doi.org/10.1016/j.tecto.2007.11.047>
- Bahrami, A., Gholamalian, H., Corradini, C., Yazdi, M., 2011a, Upper Devonian Conodont Biostratigraphy of Shams-abad section, Kerman province, Iran: *Rivista Italiana di Paleontologia e Stratigrafia*, 117(2), 199-209. <https://doi.org/10.13130/2039-4942/5971>
- Bahrami, A., Corradini, C., Yazdi, M., 2011b, Upper Devonian-Lower Carboniferous conodont biostratigraphy in the Shotori Range, Tabas area, Central-East Iran Microplate: *Bollettino della Società Paleontologica Italiana*, 50 (1), 35-53.
- Bahrami, A., Corradini, C., Over, D.J., Yazdi, M., 2013, Conodont biostratigraphy of the upper Frasnian-lower Famennian transitional deposits in the Shotori Range, Tabas area, Central-East Iran Microplate: *Bulletin of Geoscience*, 88 (2), 369-388. <https://doi.org/10.3140/bull.geosci.1353>
- Bahrami, A., Zamani, F., Corradini, C., Yazdi, M., Ameri, H., 2014a, Late Devonian (Frasnian) conodonts from the Bahram Formation in the Sar-e-Ashk Section, Kerman Province, Central East Iran Microplate: *Bollettino della*

- Società Paleontologica Italiana, 53 (3), 179-188. <https://doi.org/10.4435/BSPI.2014.15>
- Bahrami, A., Boncheva, I., Königshof, P., Yazdi, M., Ebrahimi Khan-Abadi, A., 2014b, Conodonts of the Mississippian/Pennsylvanian boundary interval in Central Iran: *Journal of Asian Earth Sciences*, 92 (1), 187-200. <https://doi.org/10.1016/j.jseas.2014.06.017>
- Bahrami, A., Königshof, P., Boncheva, I., Tabatabaei M.S., Yazdi, M., Safari, Z., 2015, Middle Devonian (Givetian) conodonts from the northern margin of Gondwana (Soh and Natanz regions, north-west Isfahan, Central Iran): biostratigraphy and paleoenvironmental implications: *Paleobiodiversity and Paleoenvironments*, 95 (4), 555-577. <https://doi.org/10.1007/s12549-015-0205-0>
- Bahrami A., Königshof, P., Vaziri-Moghaddam H., Shakeri B., Boncheva, I., 2019, Conodont stratigraphy and conodont biofacies of the shallow-water Kuh-e-Bande-Abdol-Hossein section (SE Anarak, Central Iran): *Paleobiodiversity and Paleoenvironments*, 99 (4), 477-494. <https://doi.org/10.1007/s12549-019-00384-5>
- Bahrami, A., Parast, A., Boncheva, I., Yazdi, M., 2020, Late Devonian (Famennian) conodonts from Baqer-Abad section, northeast Isfahan province, Central Iran: *Boletín de la Sociedad Geológica Mexicana*, 72 (2), 1-19. <https://doi.org/10.18268/bsgm2020v72n2a100619>
- Bahrami, A., Königshof, P., Hartkopf-Fröder, C., Kaiser, S.I., 2022, Late Devonian–Mississippian conodont biostratigraphy of the Chelcheli section, NE Shahrud (Eastern Alborz, North Iran): *Paläontologische Zeitschrift*, 96, 449-469. <https://doi.org/10.1007/s12542-021-00575-6>
- Bakhtiari, S., 2005, Road atlas of Iran Gitashenasi. Geological and Cartographic Institute, 1:1000,000: Tehran, Iran.
- Bayet-Goll, A., Moussavi-Harami, R., Mahboubi, A., 2016, Ichnotaxonomic analysis and depositional controls on the carbonate ramp ichnological characteristics of the Deh-Sufiyan Formation (Middle Cambrian), Central Alborz, Iran: *Iranian Journal of Earth Sciences*, 8 (2), 102-124.
- Becker, R.T., Kaiser, S.I., Aretz, M., 2016, Review of chrono-, litho- and biostratigraphy across the global Hangenberg Crisis and Devonian–Carboniferous Boundary, in Becker, R.T., Königshof, P., Brett, C.E. (eds.), *Devonian Climate, Sea Level and Evolutionary Events: Geological Society London, Special Publications*, 423 (1), 355-386. <https://doi.org/10.1144/sp423.10>
- Becker, R.T., Hartenfels, S., Kaiser, S.I., 2021, Review of Devonian-Carboniferous Boundary sections in the Rhenish Slate Mountains (Germany): *Palaeobiodiversity and Palaeoenvironments*, 101 (4), 357-420. <https://doi.org/10.1007/s12549-020-00469-6>
- Berberian, M., King, G.C.P., 1981, Towards a paleogeography and tectonic evolution of Iran: *Canadian Journal of Earth Sciences*, 18 (2), 210-265. <https://doi.org/10.1139/e81-019>
- Bhattacharyya, A., Chakraborty, C., 2000, *Analysis of sedimentary successions, a field manual*: Rotterdam, Brookfield, A.A. Balkema Publishers, 408 p.
- Bischoff, G., 1957, *Die Conodonten-Stratigraphie des rhenoherynischen Unterkarbons mit Berücksichtigung der Wocklumeria-Stufe und der Devon-Karbon Grenze: Abhandlungen des Hessisches Landesamt für Bodenforschung*, 84, 115-137.
- Boncheva, I., Bahrami, A., Yazdi, M., Toraby, H., 2007, Carboniferous conodont biostratigraphy and Late Paleozoic depositional evolution in south central Iran (Asadabad section, SE Isfahan): *Revista Italiana di Paleontologia e stratigrafia*, 113 (3), 329-356. <https://doi.org/10.13130/2039-4942/5879>
- Branson, E.B., 1934, Conodonts from the Hannibal Formation of Missouri: University of Missouri, Missouri.

- Branson, E.B., Mehl, M.G., 1934a, Conodonts from the Grassy Creek shale of Missouri: Missouri University Studies, 8, 171-259.
- Branson, E.B., Mehl, M.G., 1934b, Conodonts from the Bushberg sandstone and equivalent formations of Missouri: Missouri University Studies, 4, 265-300.
- Brezinski, D. K., Cecil, C.B., Skema, V.W., 2010, Late Devonian glacial and associated facies from the central Appalachian Basin, eastern United States: Geological Society of America Bulletin, 122 (1-2), 265-281. <https://doi.org/10.1130/b26556.1>
- Caputo, M.V., Melo, J.H.G., Streel, M., Isbell, J.L., 2008, Late Devonian and Early Carboniferous glacial records of South America, in Fielding, C.R., Frank, T.D., Isbell, J.L. (eds.), Resolving the Late Paleozoic Ice Age in Time and Space: Bulletin of the Geological Society of America Special Papers, 441, 161-173. [https://doi.org/10.1130/2008.2441\(11\)](https://doi.org/10.1130/2008.2441(11))
- Catuneanu, O., 2003, Sequence Stratigraphy of Clastic Systems: Geological Association of Canada, Short Course Notes. 16, 248 p.
- Catuneanu, O., Martins-Neto, M.A., Eriksson, P.G., 2005, Precambrian sequence stratigraphy: Sedimentary Geology, 176 (1-2), 67-95. <https://doi.org/10.1016/j.sedgeo.2004.12.009>
- Catuneanu, O., Abreu, V., Bhattacharya, J.P., Blum, M.D., Dalrymple, R.W., Eriksson, P.G., Fielding, C.R., Fisher, W.L., Galloway, W.E., Gibling, M.R., Giles, K.A., Holbrook, J.M., Jordan, R., Kendall, C.G.St.C., Macurda, B., Martinsen, O.J., Miall, A.D., Neal, J.E., Nummedal, D., Pomar, L., Posamentier, H.W., Pratt, B.R., Sarg, J.F., Shanley, K.W., Steel, R.J., Strasser, A., Tucker, M.E., Winker, C., 2009, Towards the standardization of sequence stratigraphy: Earth-Science Reviews, 92 (1-2), 1-33. <https://doi.org/10.1016/j.earscirev.2008.10.003>
- Chakraborty, T., Sensarma, S., 2008, Shallow marine and coastal eolian quartz arenites in the Neoproterozoic-Palaeoproterozoic Karutola Formation, Dongargarh Volcano-sedimentary succession, central India: Precambrian Research, 162 (1-2), 284-301. <https://doi.org/10.1016/j.precamres.2007.07.024>
- Chen, H.W., Lee, T.Y., Wu, L.C., 2010, High-resolution sequence stratigraphic analysis of Late Quaternary deposits of the Changhua Coastal Plain in the frontal arc-continent collision belt of Central Taiwan: Journal of Asian Earth Sciences, 39(3), 192-213. <https://doi.org/10.1016/j.jseae.2010.02.009>
- Clark, G.C., Davies, R., Hamzehpour, B., Jones, C.R., 1975, Explanatory text of the Bandar-e-Pahlavi quadrangle map. Geology Survey of Iran: Geological Quadrangle, 3, 1-198.
- Colombié, C., Strasser, A., 2005, Facies, cycles, and controls on the evolution of a keep-up carbonate platform (Kimmeridgian, Swiss Jura): Sedimentology, 52, 1207-1227. <https://doi.org/10.1111/j.1365-3091.2005.00736.x>
- Cooper, C. L., 1939, Conodonts from a Bushberg-Hannibal horizon in Oklahoma: Journal of Paleontology, 13, 379-422.
- Dorrik, A.V.S., 2010, Sedimentary Rocks in the Field: a Colour Guide: Manson Publishing Ltd, 320 p.
- Druce, E.C., 1969, Devonian and Carboniferous conodonts from Bonaparte Gulf Basin, Northern Australia. Bureau of Mineral Resources: Bulletin of Geosciences, 69, 1-243.
- Dumas, S., Arnott, R.W., 2006, Origin of hummocky and swaley cross-stratification; The controlling influence of unidirectional current strength and aggradation rate: Geology Boulder, 34 (12), 1073-1076. <https://doi.org/10.1130/G22930A.1>
- Dunham, R.J., 1962, Classification of carbonate Rocks According to Depositional texture, in Ham, W.E. (ed.), Classification of carbonate rocks. Oklahoma: Advancing the World of Petroleum Geosciences, Memoir 1, 108-121.

- Dzik, J., 2006, The Famennian “Golden Age” of conodonts and ammonoids in the Polish part of the Variscan Sea: *Acta Palaeontologica Polonica*, 63, 1-359.
- Einsle, G., 2000, *Sedimentary Basins: Evolution: Facies, and Sediment Budget*: Springer Verlag, Heidelberg, 792 p. <http://dx.doi.org/10.1007/978-3-662-04029-4>
- Embry, A.F., Klovan, J.E., 1971, A Late Devonian reef tract on northeastern Banks Island: The Northwest Territories: *Bulletin of Canadian Petroleum Geology*, 19 (4), 730-781. <https://doi.org/10.35767/gscpgbull.19.4.730>
- Emery, D., Myers, K.J., 1996, *Sequence Stratigraphy*: Oxford, U. K., Blackwell Science, 297 p. <http://dx.doi.org/10.1002/9781444313710>
- Epstein, A.G., Epstein, J.B., Harris, L.D., 1977, Conodont color Alteration; an index to Organic Metamorphism: Geological Survey Professional paper, 995, 1-27. <https://doi.org/10.3133/pp995>
- Ernst, A., Königshof, P., Bahrami, A., Yazdi, M., Boncheva, I., 2016, A Late Devonian (Frasnian) bryozoan fauna from central Iran: *Palaeobiodiversity and Palaeoenvironments*, 97 (3), 541-552. <https://doi.org/10.1007/s12549-016-0269-5>
- Ernst, A., Bahrami, A., Parast, A., 2020, Early Famennian bryozoan from the Baqer-abad section, northeast Isfahan, central Iran: *Palaeobiodiversity and Palaeoenvironments*, 100 (1-2), 705-718. <https://doi.org/10.1007/s12549-020-00417-4>
- Flügel, E., 2010, *Microfacies of Carbonate Rocks, Analysis Interpretation and Application*: Springer, Berlin, 976 p.
- Foix, N., Paredes, J.M., Giacosa, R.E., 2013, Fluvial architecture variations linked to changes in accommodation space: Río Chico Formation (Late Paleocene), Golfo San Jorge basin, Argentina: *Sedimentary Geology*, 294, 342-355. <https://doi.org/10.1016/j.sedgeo.2013.07.001>
- Ghorbani, M., Rostamnejad, A., Valiani Z., 2014, Microfacies, petrofacies and sedimentary environment of the Bahram Formation in Hutk section (Northern Kerman), Iran: *International Journal of Geology, Earth and Environmental Sciences*, 4(1), 68-84.
- Ghosh, P., Sarkar, S., Maulik, P., 2006, Sedimentology of a muddy alluvial deposit: Triassic Denwa Formation, India: *Sedimentary Geology*, 191 (1-2), 3-36. <https://doi.org/10.1016/j.sedgeo.2006.01.002>
- Golonka, J., 2007, Phanerozoic paleoenvironment and paleolithofacies maps: late Paleozoic: *Geologia*, 33 (2), 145-209.
- Haq, B.U., Schalteer, S.R., 2008, A Chronology of Paleozoic Sea-Level Changes: *Science*, 322, 64-68. <https://doi.org/10.1126/science.1161648>
- Harms, J.C., Southard, J.B. Walker, R.G., 1982, Structures and Sequence in Clastic Rocks. Lecture Notes: Society Economic Paleontologist and Mineralogists Short Course, 9, 55 p. <https://doi.org/10.2110/scn.82.09>
- Helms, J., 1959, Conodonten aus dem Saalfelder Oberdevon (Thuringen): *Geologie*, 8, 634-677.
- Higgs, K.E., King, P.R., Raince, J.I., Sykes, R., Browne, G.H., Crouch, E.M., Baur, J.R., 2012, Sequence stratigraphy and controls on reservoir sandstone distribution in an Eocene marginal marine-coastal plain fairway, Taranaki Basin, New Zealand: *Marine and Petroleum Geology*, 32 (1), 110-137. <https://doi.org/10.1016/j.marpetgeo.2011.12.001>
- Huddle, J. W., 1934, Conodonts from the New Albany Shale of Indiana: *Bulletins of American paleontology*, 21, 1-136.
- Hüneke, H., 2001, Gravitative und strömungsinduzierte Resedimente devonischer Karbonatabfolgen im marokkanischen Zentralmassiv (Rabat-Tiflet-Zone, Decke von Ziar-Mrirt): Professoral diss., University of Greifswald, 227 p.
- Hunt, D., Tucker, M.E., 1992, Stranded parasequences and the forced regressive

- wedge systems tract: deposition during base-level fall: *Sedimentary Geology*, 81 (1-2), 1-9. [https://doi.org/10.1016/0037-0738\(92\)90052-S](https://doi.org/10.1016/0037-0738(92)90052-S)
- Ichaso, A., Dalrymple, R.W., 2006, Abstracts with Programs. On the Geometry of Tidalmeanders: *Geological Society of America Bulletin*, 7, 38, 186.
- Isaacson, P.E., Hladil, J., Shen, J., Kalvoda, J., Grader, G., 1999, Late Devonian (Famennian) glaciation in South America and marine offlap on other continents: *Abhandlungen-Geologischen Bundesanstalt*, 54, 239-258.
- Isaacson, P.E., Diaz-Martinez, E., Grader, G.W., Kalvoda, J., Babek, O., Devuyt, F.X., 2008, Late Devonian–earliest Mississippian glaciation in Gondwanaland and its biogeographic consequences: *Palaeogeography, Palaeoclimatology, Palaeoecology*, 268 (3-4), 126-142. <https://doi.org/10.1016/j.palaeo.2008.03.047> [Get rights and content](#)
- Jeppsson, L., Anehus, R., 1995, A buffered formic-acid technique for conodont extraction: *Journal of Paleontology*, 69 (4), 790-794. <https://doi.org/10.1017/s0022336000035319>
- Johnson, J., Klapper, G., Sandberg, C.A., 1985, Devonian eustatic fluctuations in Euramerica: *Geological Society of America Bulletin*, 96 (5), 567-587. [https://doi.org/10.1130/0016-7606\(1985\)96<567:dfic>2.0.co;2](https://doi.org/10.1130/0016-7606(1985)96<567:dfic>2.0.co;2)
- Kaiser, S.I., Becker, R.T., Spalletta, C., Steuber, T., 2009, High-resolution conodont stratigraphy, biofacies and extinctions around the Hangenberg Event in pelagic successions from Austria, Italy and France, in Over, D.J. (ed.), *Studies in Devonian Stratigraphy: Proceedings of the 2007 International Meeting of the Subcommission on Devonian Stratigraphy and IGCP 499: Palaeontographica Americana*, 63, 99-143. _
- Kaiser S.I., Corradini, C., 2011, The early siphonodellids (Conodonta, Late Devonian–Early Carboniferous): overview and taxonomic state: *Neues Jahrbuch für Geologie und Paläontologie*, 261 (1), 19-35. <https://doi.org/10.1127/0077-7749/2011/0144>
- Kaiser, S.I., Aretz, M., Becker, R.T., 2016, The global Hangenberg Crisis (Devonian–Carboniferous transition): review of a first-order mass extinction, in Becker, R.T., Königshof, P., Brett, C.E. (eds.), *Devonian climate, sea level and evolutionary events: Geological Society London, Special Publications*, 423, 387-437. <https://doi.org/10.1144/SP423.9>
- Kaiser, S. I., Kumpan, T., and Cígler, V., 2017, New unornamented siphonodellids (Conodonta) of the lower Tournaisian from the Rhenish Massif and Moravian Karst (Germany and Czech Republic): *Neues Jahrbuch für Geologie und Paläontologie, Abhandlungen*, 286 (1), 1-33. <https://doi.org/10.1127/njgpa/2017/0684>
- Khalifa, M.A., Catuneanu, O., 2008, Sedimentology of the fluvial and fluvio-marine facies of the Bahariya Formation (Early Cenomanian), Bahariya Oasis, Western Desert, Egypt: *Journal of African Earth Sciences*, 51 (2), 89-103. <https://doi.org/10.1016/j.jafrearsci.2007.12.004>
- Königshof, P., Carmichael, S., Waters, J., Jansen, U., Bahrami, A., Boncheva, I., Yazdi, M., 2017, Palaeoenvironmental study of the Paleotethys Ocean: The Givetian-Frasnian boundary of a shallow-marine environment using combined facies analysis and geochemistry (Zefreh Section/Central Iran): *Palaeobiodiversity and Palaeoenvironments*, 97 (3), 517-540. <https://doi.org/10.1007/s12549-016-0253-0>
- Königshof, P., Bahrami, A., Kaiser, S.I., 2021, Devonian-Carboniferous boundary sections in Iran: *Palaeobiodiversity and Palaeoenvironments*, 101 (2), 613-632. <https://doi.org/10.1007/s12549-020-00438-z>
- Lakin, J.A., Marshall, J.E.A., Troth, I., Harding, I.C., 2016, Greenhouse to icehouse: a

- biostratigraphic review of latest Devonian–Mississippian glaciations and their global effects, in: Becker, R.T., Königshof, P., Brett, C.E. (eds.), Devonian climate, sea level and evolutionary events: Geological Society London, Special Publications, 423, 439-464. <https://doi.org/10.1144/sp423.12>
- Lane, H.R., Sandberg, C., Ziegler, W., 1980, Taxonomy and phylogeny of some Lower Carboniferous conodonts and preliminary standard post – Siphonodella zonation: *Geologica et Paleontologica*, 14, 117-164.
- Lane, H.R., Ziegler, W., 1983, Taxonomy and phylogeny of *Scaliognathus* Branson and Mehl, 1941 (Conodonts, Lower Carboniferous). *Senckenbergiana lethaea* 64 (2-), 199-225.
- Lewin, J., Ashworth, P.J., 2014, Defining large river channel patterns: Alluvial exchange and plurality: *Geomorphology*, 250, 83-98. <https://doi.org/10.1016/j.geomorph.2013.02.024>
- Longhitano, S.G., Mellere, D., Steel, R.J., Ainsworth, R.B., 2012, Tidal depositional systems in the rock record: A review and new insights: *Sedimentary Geology*, 279, 2-22. <https://doi.org/10.1016/j.sedgeo.2012.03.024>
- Machel, H.G., Hunter, I.G., 1994, Facies model for Middle to Late Devonian shallow-marine carbonates, with comparisons to modern reefs: a guide for facies analysis: *Facies*, 30, 155-176. <https://doi.org/10.1007/bf02536895>
- Mack, G.H., James, W.C., 1992, *Paleosols for Sedimentologists: Short Course Notes*: Geological Society of America, New York, 127 p.
- Mehl, M.G., Thomas, L.A., 1974, Conodonts from the Fern Glen of Missouri. *J. Sci. Lab. Denison Univ.* 40, 3-20.
- Miall, A.D., 2006, *The Geology of Fluvial Deposits: Sedimentary Facies, Basin Analysis, and Petroleum Geology*: Springer-Verlag, New York, 582 p.
- Moslow, T.F., Tye, R.S., 1985, Recognition and characterization of Holocene tidal inlet sequences: *Marine Geology*, 63 (1-4), 129-151. [https://doi.org/10.1016/0025-3227\(85\)90081-7](https://doi.org/10.1016/0025-3227(85)90081-7)
- Muttoni, G., Mattei, M., Balini, M., Zanchi, A., Gaetani, M., Berra, F., 2009, The drift history of Iran from the Ordovician to the Triassic, in Brunet, M.F., Wilmsen, M., Granath, J.W. (eds.), *South Caspian to Central Iran Basins*: Geological Society, London, Special Publication, 312, 7-29. <https://doi.org/10.1144/sp312.2>
- Myrow, P.M., Ramezani, J., Hanson, A.E., Bowring, S.A., Racki, G., Rakociński, M., 2014, High-precision U-Pb age and duration of the latest Devonian (Famennian) Hangenberg Event, and its implications: *Terra Nova*, 26 (3), 222-229. <https://doi.org/10.1111/ter.12090>
- Najjarzadeh, M.T., 1998, *Biostratigraphy of the Devonian strata on based of Conodonts elements in Zoo section (Eastern Alborz), Iran*. University of Ferdowsi, Iran, M.Sc. Thesis, (in Persian).
- Najjarzadeh, M.T., Ashouri, A.R., Yazdi, M., Bahrami, A., 2020, Biostratigraphy of Devonian-Carboniferous boundary in Tuyeh-Darvar section, north of Iran: *Iranian Journal of Earth Sciences* 12 (2), 98-123. <https://doi.org/10.30495/IJES.2020.673332>
- Nogol-e-Sadat, M.A.A., Almasian, M., 1993, *Tectonic Map of Iran, Scale: 1/1000000: Treatise on the geology of Iran*, Geological Survey of Iran.
- Omali, A.O., Imasuen, O.I., Okiotor, M.E., 2011, Sedimentological Characteristics of Lokoja Sandstone Exposed At Mount Patti, Bida Basin: Nigeria. *Advances in Applied Science Research*, 2 (2), 227-245.
- Parvizi, T., Bahrami, A., Königshof, P., Kaiser, S., 2021, Conodont biostratigraphy of Upper Devonian–Lower Carboniferous deposits in eastern Alborz (Mighan section), North Iran: *Palaeoworld*, 31 (1), 69-85. <https://doi.org/10.1016/j.palwor.2021.01.008>

- Perri, M.C., Spalletta, C., 1990, Famennian conodonts from climenid pelagic limestone, Carnic Alps, Italy: *Palaeontographia Italica*, 77, 55-83.
- Pettijohn, F.J., Potter, P.E., Siever, R., 1987, *Sand and Sandstone*: Springer, New York. 553 p. <http://dx.doi.org/10.1007/978-1-4612-1066-5>
- Reineck, H.E., Singh, I.B., 1980, *Depositional Sedimentary Environment: With Reference to Terrigenous Clastics*: Springer-Verlag, Berlin Heidelberg New York, 439 p.
- Rhodes, F.H.T., Austin, R.L., Druce, E.C., 1969, British Avonian (Carboniferous) Conodont Faunas, and their Value in Local and Intercontinental Correlation: *Bulletin of the Natural History Museum, London, Geology and Paleontology*, 5, 313 p.
- Saidi, A., Akbarpour, M.R., 1992, Geological Map of Iran. 1:100,000 series, sheet No. 676, Kiyasar. Geological survey of Iran, Tehran.
- Salehi, M.A., Bahrami, A., Moharrami, S., Vaziri-Moghaddam, H., Pakzad, H.R., Shakeri, B., 2020, Palaeoenvironmental and sequence-stratigraphic analysis of the Middle-Late Devonian carbonates (Bahram Formation) of Anarak, western Central Iran: *Journal of African Earth Sciences*, 171 (103938), 1-18. <https://doi.org/10.1016/j.jafrearsci.2020.103938>
- Sandberg, C.A., Streeck, M., Scott, R.A., 1972, Comparison between conodont zonation and spore assemblages at the Devonian-Carboniferous boundary in the western and central United States and in Europe, in *Congres International de Stratigraphie et de Géologie Du Carbonifère*, Krefeld, 179-203.
- Sandberg, C.A., Ziegler, W., Leuteritz, K., Brill, S.M., 1978, Phylogeny, speciation, and zonation of *Siphonodella* (Conodonta, Upper Devonian and Lower Carboniferous): *Newsletter On Stratigraphy*. 7 (2), 102-120. <https://doi.org/10.1127/nos/7/1978/102>
- Sattari, E., Bahrami, A., Königshof, P., Vaziri-Moghaddam, H., 2021, Late Devonian (Famennian) to Carboniferous (Mississippian-Pennsylvanian) conodonts from the Anarak section, Central Iran: *Paleobiodiversity and paleoenvironments*, 101,781-802. <https://doi.org/10.1007/s12549-020-00462-z>
- Sattari, E., Bahrami, A., Vaziri-Moghaddam, H., Taheri, A., Boncheva, I., 2023, Biostratigraphy, Microfacies, Sedimentary Environments and Sequence Stratigraphy of the Late Devonian-Carboniferous Deposits at the Anarak Section: Central Iran, *Acta Geologica Sinica*, 97 (4), 1038-1057. <https://doi.org/10.1111/1755-6724.15071>
- Scotese, C.R. 2001, *Atlas of Earth-History. Paleogeography*, vol. 1. Arlington: Paleomap Project.
- Selley, R.C., 2000, *Applied sedimentology*: Academic Press, San Diego California, 523p.
- Şengör, A.M.C., Altiner, D., Cin, A., Ustaömer, T., Hsü, K.J., 1988, Origin and assembly of the Tethyside orogenic collage at the expense of Gondwana Land: *Geological Society, London, Special Publications*, 37 (1), 119-181. <https://doi.org/10.1144/gsl.sp.1988.037.01.09>
- Sharafi, M., Mahboubi, A., Moussavi-Harami, R., Mosaddegh, H., Gharaie, M.H.M., 2014, Trace fossils analysis of fluvial to open marine transitional sediments: Example from the Upper Devonian (Geirud Formation), Central Alborz, Iran: *Palaeoworld*, 23 (1), 50-68. <https://doi.org/10.1016/j.palwor.2013.10.004>
- Sharafi, M., Longhitano, S.G., Mahboubi, A., Moussavi-Harami, R., Mosaddegh, H., 2016, Sedimentology of a transgressive mixed-energy (wave/tide-dominated) estuary, Upper Devonian Geirudn Formation (Alborz Basin, northern Iran), in Tessier, B., Reynaud, J.-Y. (eds), *Contributions to Modern and Ancient Tidal Sedimentology: Proceedings of the Tidalites 2012 conference*, Wiley, 261-292. <https://doi.org/10.1002/9781119218395.ch15>

- Shinn, E.A., 1983, Tidal flat environment, in Scholle, P.A., Bebout, D.G., Moore, C.H. (Eds.), Carbonate Depositional Environments. AAPG Memoir, 173-210.
- Shinn, E.A., 1986, Modern Carbonate Tidal Flats: Their Diagnostic Features. Colorado-School of Mines Quarterly, 81, 7-35.
- Sorkhabi, R., Macfarlane, A., 1999, Himalaya and Tibet: Mountain roots to mountain tops, in Macfarlane, A., Sorkhabi, R.B, and Quade, J. (eds.), Himalaya and Tibet: Mountain Roots to Mountain Tops: Geological Survey of America, Special Paper, 328, 1-8. <https://doi.org/10.1130/0-8137-2328-0.1>
- Spalletta, C., Perri, M.C., Over, D.J., Corradini, C., 2017, Famennian (Upper Devonian) conodont zonation: revised global standard: Bulletin of Geosciences, 92 (1), 31-57. <https://doi.org/10.3140/bull.geosci.1623>
- Stampfli, G.M., Mosar, J., Favre, P., Pillevuit, A., Vannay, J.C., 2001, Permo-Mesozoic evolution of the western Tethys realm: The Neo-Tethys East Mediterranean Basin connection, in Ziegler, P.A., Cavazza, W., Robertson, A.H.F., Crasquin-Soleau, S. (eds.), Peri-Tethys Memoir 6: Peri-Tethyan Rift/Wrench Basins and Passive Margins: Mémoires du Muséum National d'Histoire Naturelle, Paris, 186, 51-108
- Stöcklin, J., 1968, Structural History and Tectonics of Iran: A Review: Advancing the World of Petroleum Geosciences Bulletin 52 (7), 1229-1258. <https://doi.org/10.1306/5D25C4A5-16C1-11D7-8645000102C1865D>
- Stöcklin, J., 1974, Possible Ancient Continental Margins in Iran, in Burk, C.A., Drake, C.L. (eds.), The Geology of Continental Margins: Springer, Berlin, Heidelberg, 873-887. https://doi.org/10.1007/978-3-662-01141-6_64
- Strand, K., 2005, Sequence stratigraphy of the siliciclastic East Puolanka Group, the Palaeoproterozoic Kainuu Belt, Finland: Sedimentary Geology, 176 (1-2), 149-166. <https://doi.org/10.1016/j.sedgeo.2004.12.014>
- Streel, M., Caputo, M.V., Loboziak, S., Melo, J.H.G., 2000a, Late Frasnian–Famennian climates based on palynomorph analyses and the question of the Late Devonian glaciations: Earth-Science Reviews, 52 (1-3), 121-173. [https://doi.org/10.1016/S0012-8252\(00\)00026-X](https://doi.org/10.1016/S0012-8252(00)00026-X)
- Streel, M., Thorez, J., Caputo, M.V., Loboziak, S., Melo, J.H.G., 2000b, Palynology and sedimentology of laminites and tillites from the latest Famennian of the Parnaíba Basin, Brazil: Geologica Belgica, 3 (1–2), 87-96. <https://doi.org/10.20341/gb.2014.025>
- Thompson, T.L., Fellows, L.D., 1970, Stratigraphy and conodont biostratigraphy of Kinderhookian and Osagian (Lower Mississippian) Rocks of southwestern Missouri and adjacent areas: Missouri Geological Survey and Water Resources, 45, 1-263.
- Tucker, M.E., Wright V.P., 1990, Carbonate Sedimentology: Blackwell Scientific Publications, Oxford, 482 p. <http://dx.doi.org/10.1002/9781444314175>
- Tucker, M.E., 2001, Sedimentary Petrology: Blackwell, Oxford, 260 p.
- Vakarelov, B.K., Ainsworth, R.B., MacEachern, J.A., 2012, Recognition of wave-dominated, tide influenced shoreline systems in the rock record: Variations from a microtidal shoreline model: Sedimentary Geology, 279, 23-41. <https://doi.org/10.1016/j.sedgeo.2011.03.004>
- Uchman, A., Krenmayr, H.G., 2004, Trace fossils, ichnofabrics and sedimentary facies in the shallow marine Lower Miocene Molasse of Upper Austria: Jahrbuch der Geologischen Bundesanstalt, 144 (2), 233-251.
- Ulrich, E. O., Bassler, R. S., 1926, A classification of the toothlike fossils, conodonts, with descriptions of American Devonian and Mississippian species: USNM., 68, 63 p. <https://doi.org/10.5479/si.00963801.68-2613.1>

- Wendt, J., Kaufmann, B., Belka, Z., Farsan, N., Karimi Bavandpur, A., 2005, Devonian/Lower Carboniferous stratigraphy, facies patterns and palaeogeography of Iran. Part II. Northern and central Iran: Acta Geologica Polonica, 55 (1), 31-97.
- Zamani, F., Yazdi, M., Bahrami, A., Girard, C., Spalletta, C., Ameri, H., 2021, Middle Givetian to late Famennian (Middle to Late Devonian) conodonts from the northern margin of Gondwana (Kerman region, Central Iran): Historical Biology, 33 (11), 2591-2609. <https://doi.org/10.1080/08912963.2020.1819997>
- Zand-Moghaddam, H., Moussavi-Harami, R., Mahboubi, A., 2014, Sequence stratigraphy of the Early–Middle Devonian succession (Padeha Formation) in Tabas Block, East-Central Iran: Implication for mixed tidal flat deposits: Palaeoworld, 23 (1), 31-49. <https://doi.org/10.1016/j.palwor.2013.06.002>
- Ziegler, W., 1962, Taxionomie and Phylogenie Oberdevonischer Conodonten und ihre stratigraphische Bedeutung: Abhandlungen Des Hessischen Landesamts Für Bodenforschung, 38, 166 p.
- Ziegler, W., 1969, Eine neue Conodonten fauna aus dem höchsten Oberdevon: Fortschritte Geologie von Rheinland und Westfalen, 17, 179-191.
- Ziegler, W., Sandberg, C.A., Austin, R.L., 1974, Revision of *Bispathodus* group (Conodonta) in the Upper Devonian and Lower Carboniferous: Geologica et Paleontologica, 8, 97-112.
- Ziegler, W., Sandberg, C.A., 1990, The Late Devonian Standard Conodont Zonation: Courier Forschungsinstitut Senckenberg, 121, 1-115.
- Zonneveld, J.-P., Gingras, M.K., Pemberton, S.G., 2001, Trace fossil assemblages in a Middle Triassic mixed siliciclastic-carbonate marginal marine depositional system, British Columbia: Palaeogeography, Palaeoclimatology, Palaeoecology, 166 (3-4), 249-279. [https://doi.org/10.1016/s0031-0182\(00\)00212-1](https://doi.org/10.1016/s0031-0182(00)00212-1)

Appendix 1

Figure 5 - Conodonts from the Tuye-Darvar section, the scale bar is 100 μ m.

1, 7, 10, 11, 15, 22, 23, 24- *Pseudopolygnathus multistriatus* Branson and Mehl, 1934b; 1- Upper view of IUMC 300, sample S27; 7- Upper lateral view of IUMC 306, sample S27; 10- Upper view of IUMC 311, sample S29; 11- Upper view of IUMC 312, sample S31; 15- Upper view of IUMC 313, sample S32; 22- Upper view of IUMC 327, sample S27; 23- Upper view of IUMC 328, sample S26; 24- Upper view of IUMC 336, sample S26. **2, 6, 16, 17, 18, 19, 27- *Pseudopolygnathus primus*** Branson and Mehl, 1934; 2- Upper view of IUMC 301, sample S10; 6- Upper view of IUMC 301, sample S10; 16- Upper view of IUMC 315, sample S11; 17- Upper view of IUMC 317, sample S12; 18- Upper view of IUMC 321, sample S12; 19- Upper view of IUMC 322, sample S13; 27- Upper view of IUMC 322, sample S13. **3, 20, 21, 25, 26, 28, 29- *Bispathodus aculeatus aculeatus*** Branson and Mehl, 1934a; 3- Upper lateral view of IUMC 302, sample S6; 20- Upper view of IUMC 323, sample S6; 21- Upper view of IUMC 326, sample S6; 25- Upper view of IUMC 335, sample S7; 26- Upper view of IUMC 338, sample S7; 28- Upper view of IUMC 338, sample S8; 29- Upper view of IUMC 338, sample S8. **4, 14, 38- *Bispathodus aculeatus plumulus*** (Rhodes et al., 1969); 4- Upper lateral view of IUMC 303, sample S92; 14- Upper lateral view of IUMC 303, sample S92; 38- Upper lateral view of IUMC 303, sample S92. **5- *Bispathodus spinolicostatus*** Branson, 1934; Upper lateral view of IUMC 304, sample S14. **8, 12, 14- *Bispathodus aculeatus aculeatus*** Branson and Mehl, 1934a; 8- Upper lateral view of IUMC 307, sample S6; 12- Upper lateral view of IUMC 310, sample S7; 14- Upper view of IUMC 314, sample S9. **9- *Pseudopolygnathus dentilineatus*** Branson, 1934; Upper view of IUMC 308, sample S26. **13- *Clydagnathus plumulus*** (Rhodes et al., 1969); Upper view of IUMC 309, sample S8. **30, 31, 33- *Bispathodus stabilis vulgaris*** (Dzik, 2006) [M1]; 30- Upper view of IUMC 309, sample S16; 31- Upper view of IUMC 309, sample S16; 33- Upper view of IUMC 309, sample S18. **32- *Bispathodus stabilis bituberculatus*** (Dzik, 2006) [M3]; Upper view of IUMC 390, sample S6. **34, 35, 36- *Branmehla inornata*** (Branson and Mehl, 1934a); 34- Upper view of IUMC 309, sample S7; 35- Upper view of IUMC 309, sample S7; 36- Upper view of IUMC 309, sample S8. **37- *Bispathodus stabilis stabilis*** (Branson and Mehl, 1934a) [M2]; Upper view of IUMC 309, sample S20. **39, 40, 41, 42, 43- *Bispathodus stabilis vulgaris*** (Dzik, 2006) [M1]; 39- Upper view of IUMC 309, sample S16; 40- Upper view of IUMC 309, sample S16; 41- Upper view of IUMC 309, sample S18; 42- Upper view of IUMC 309, sample S14; 43- Upper view of IUMC 309, sample S14. **44- *Bispathodus bispathodus*** Ziegler et al., 1974; Upper view of IUMC 309, sample S8. **45, 46- *Polygnathus communis communis*** Branson and Mehl, 1934b; 45- Upper view of IUMC 309, sample S24; 46- Upper view of IUMC 309, sample S25. **47-53- *Polygnathus communis dentatus*** Druce 1969; 47- Upper view of IUMC 316, sample S17; 48- Upper view of IUMC 334, sample S17; 49- Upper view of IUMC 316, sample S19; 50- Upper view of IUMC 334, sample S19; 51- Upper view of IUMC 316, sample S21; 52- Upper view of IUMC 334, sample S21; 53- Upper view of IUMC 334, sample S21. **54- *Polygnathus inornatus inornatus*** Branson, 1934; Upper view of IUMC 334, sample S30. **55- *Polygnathus semicostatus*** Branson and Mehl, 1934; Upper view of IUMC 334, sample S8. **56- *Scaphignathus velifer velifer*** Helms, 1959; Upper view of IUMC 334, sample S2. **57- *Polygnathus delicatulus*** Ulrich and Bassler, 1926; Upper (a) and Lower (b) views of IUMC 316, sample S6. **58- *Polygnathus padovanii*** Perri and Spalletta 1990; Upper view of IUMC 316, sample S2. **59- *Polygnathus inornatus inornatus*** Branson, 1934; Upper view of IUMC 316, sample S33. **60, 61- *Bispathodus jugosus*** (Branson and Mehl, 1934a); 60- Upper view of IUMC 316, sample S7; 61- Upper view of IUMC 334, sample S9. **62- *Bispathodus ultimus*** M1 Bischoff, 1957; Upper view of IUMC 316, sample S8.

Appendix 2

Figure 6- Conodonts from the Tuye-Darvar section, the scale bar is 100 μ m.

1- *Bispathodus stabilis vulgaris* (Dzik, 2006) [M1]; Upper view of IUMC 309, sample S8. **2- *Bispathodus bispathodus*** Ziegler et al., 1974; Upper view of IUMC 309, sample S5. **3- *Bispathodus costatus*** (Branson 1934) Morphotype 2; Upper view of IUMC 309, sample S9. **4, 8- *Bispathodus jugosus*** (Branson and Mehl 1934a); 4- Upper view of IUMC 309, sample S5; 8- Upper view of IUMC 309, sample S7. **5- *Bispathodus aculeatus aculeatus*** Branson and Mehl, 1934a; Upper view of IUMC 309, sample S8. **6- *Palmatolepis minuta minuta*** Branson and Mehl 1934a; Upper view of IUMC 309, sample S2. **7- *Bispathodus aculeatus aculeatus*** Branson and Mehl, 1934a; Upper view of IUMC 309, sample S9. **9, 10, 20- *Polygnathus inornatus*** Rhodes et al., 1969; 9- Upper (a) and lower (b) views of IUMC 334, sample S26; 10- Upper (a) and lower (b) views of IUMC 334, sample S27; 20- Upper (a) and lower (b) views of IUMC 334, sample S28. **11, 12, 15, 17- *Siphonodella praesulcata*** M2 Sandberg, 1972; 11- Upper view of IUMC 316, sample S10; 12- Upper view of IUMC 334, sample S10; 15- Upper view of IUMC 316, sample S14; 17- Upper view of IUMC 334, sample S16. **13, 16, 19- *Siphonodella sulcata*** Huddle, 1934; 13- Upper view of IUMC 316, sample S16; 16- Upper view of IUMC 334, sample S16; 19- Upper view of IUMC 316, sample S20. **14- *Polygnathus communis communis*** Branson and Mehl, 1934b; Upper view of IUMC 309, sample S25. **26, 27, 29, 30, 32, 35- *Gnathodus pseudosemiglaber*** Thompson and Fellow, 1970; 26- Upper view of IUMC 316, sample S37; 27- Upper view of IUMC 334, sample S37; 29- Upper view of IUMC 316, sample S38; 30- Upper view of IUMC 316, sample S38; 32- Upper view of IUMC 334, sample S40; 35- Upper view of IUMC 316, sample S40. **31, 37- *Gnathodus cueneiformis*** Mehl and Thomas, 1974; 31- Upper view of IUMC 334, sample S26; 37- Upper view of IUMC 316, sample S27. **33, 38- *Gnathodus typicus*** Cooper, 1939; 33-Upper view of IUMC 334, sample S34; 38- Upper view of IUMC 334, sample S34. **39, 40, 41- *Pseudopolygnathus cf. oxypageus*** Lane et al., 1980; 39- Upper view of IUMC 334, sample S39; 40- Upper view of IUMC 316, sample S39; 41- Upper view of IUMC 334, sample S40. **24, 34, 36- *Gnathodus semiglaber*** Bischoff, 1957; 24-Upper view of IUMC 334, sample S37; 34-Upper view of IUMC 334, sample S37; 36-Upper view of IUMC 334, sample S38. **18, 21- *Polygnathus longiposticus*** Branson and Mehl, 1934; 18- Upper view of IUMC 334, sample S26; 21- Upper view of IUMC 334, sample S26. **23, 25- *Protognathodus collinsoni*** Ziegler, 1969; 23- Upper view of IUMC 334, sample S17; 25- Upper view of IUMC 334, sample S20. **28- *Protognathodus kockeli*** (Bischoff, 1957); Upper view of IUMC 334, sample S20. **22- *Protognathodus meischneri*** Ziegler, 1969; Upper view of IUMC 334, sample S17.